+

Investigation of *Medicago truncatula* genes' involvement in arbuscular mycorrhizal symbiosis

Téa Backlund

Thesis submitted to the
University of Ottawa
In partial fulfillment of the requirements for the
Master of Science in Biology

Department of Biology
Faculty of Science
University of Ottawa

ABSTRACT

The mutualistic associations between Arbuscular mycorrhizal (AM) fungi and plant roots are ancient and ubiquitous across the plant kingdom, where AM fungi provide Phosphorus, Nitrogen, and water to the plant, and receive photosynthetically fixed Carbon in the form of fatty acids and sugars in return. Moreover, AM fungi are associated with increased plant resistance to both abiotic and biotic stressors such as drought and viral pathogens. Frequently used in agriculture, AM fungi are observed to increase crop yields and decrease chemical fertilizer needs for many economically important plant species. The potential to increase AM fungal effectiveness remains a driving force for current research. To determine their role in establishing and/or supporting AM symbiosis, we propose a reverse genetic study of two genes in the model legume *Medicago truncatula*. Based on RNA sequencing data indicating increased expression during AM symbiosis, we selected one gene that encodes for NAC TF-like protein, which belongs to a large family of plant transcription factors primarily involved in regulating the secretion of defence hormones. The second gene selected, *PALM1*, was recently discovered to play a role in the regulation of the trifoliate leaf structure of *M. truncatula*. We hypothesize that the genes under study play mechanistic roles in regulating AM fungal symbiosis and that we will observe a difference between the colonization rates of corresponding gene mutants and control groups. Firstly, we explored the involvement of the *PALM1* and NAC TF genes by examining the root developmental phenotype of *Medicago truncatula* mutants. Secondly, we employed symbiosis assays to investigate the colonization rates of the genes in question. Results indicated that the NAC TF gene had no consistent role in the AM symbiosis, while the *PALM1* gene revealed promising results, where significant increases in colonization rates were observed in *PALM1* mutants throughout repeated experiments. Future research involves using this study to help pursue more effective ways to use AM fungi symbiosis in sustainable agro ecosystems.

RÉSUMÉ

Les associations mutualistes entre les champignons mycorhiziens arbusculaires (AM) et les racines des plantes sont anciennes et omniprésentes dans le règne végétal, où les champignons AM fournissent du phosphore, de l'azote et de l'eau à la plante, et reçoivent du carbone fixé par photosynthèse sous forme d'acides gras et de sucres dans revenir. De plus, les champignons AM sont associés à une résistance accrue des plantes aux facteurs de stress abiotiques et biotiques tels que la sécheresse et les agents pathogènes viraux. Fréquemment utilisés en agriculture, on observe que les champignons AM augmentent les rendements des cultures et diminuent les besoins en engrais chimiques pour de nombreuses espèces végétales économiquement importantes. Le potentiel d'augmentation de l'efficacité fongique AM reste une force motrice pour la recherche actuelle. Afin de déterminer leur rôle dans l'établissement et/ou le soutien de la symbiose AM, nous proposons une étude de génétique inverse de deux gènes chez la légumineuse modèle Medicago truncatula. Sur la base de données de séquençage d'ARN indiquant une expression accrue lors de la symbiose AM, nous avons sélectionné un gène qui code pour la protéine de type NAC TF, qui appartient à une grande famille de facteurs de transcription végétaux principalement impliqués dans la sécrétion d'hormones de défense. Le deuxième gène sélectionné, *PALM1*, a récemment été découvert comme jouant un rôle dans la régulation de la structure des feuilles trifoliées de M. truncatula. Nous émettons l'hypothèse que les gènes à l'étude jouent des rôles mécanistes dans la régulation de la symbiose fongique AM, et que nous observerons une différence entre les taux de colonisation des groupes mutants et témoins. Tout d'abord, nous avons exploré l'implication des gènes *PALM1* et NAC TF en examinant le phénotype des mutants de Medicago truncatula. Deuxièmement, nous avons utilisé des tests de symbioses pour étudier les taux de colonisation des gènes en question. Les résultats ont indiqué que le gène de type NAC TF n'avait pas de rôle constant dans la symbiose AM, tandis que le gène *PALM1* a révélé des résultats prometteurs, où des augmentations significatives des taux de colonisation ont été observées tout au long d'expériences répétées. Les recherches futures impliquent l'utilisation de cette étude pour aider à rechercher des moyens plus efficaces d'utiliser la symbiose des champignons AM dans des agro-écosystèmes durables.

ACKNOWLEDGEMENTS

I wish to express my deepest gratitude to my supervisor, Dr. Allyson MacLean, for her expertise and guidance throughout my extended time in her laboratory. I am grateful for her patience, encouragement, and kindness. I would like to thank her for the opportunity to conduct such exciting research under the supervision of such a brilliant scientist. I am also grateful for the assistance and understanding I received from the members of my thesis advisory committee, Dr. Martha Mullaly, and Dr. Marina Cvetkovska.

I would like to convey my sincere appreciation to Laboratory Technician Mina Nasr-Sharif, for her extraordinary help and counsel throughout my project. The passion that she conveys for her research is inspiring, and the leadership she demonstrates in the laboratory is exemplary. I would also like to give thanks to all the past and present students and post-docs of the MacLean lab for their friendship and support throughout my time in the laboratory.

I am indebted to the Faculty of Science staff. My project would not have been possible without the many people who maintain the autoclave services, the common laboratory facilities, the growth chambers, the Science Store, and the Graduate Studies Offices.

I would like to thank my friends, parents, and my partner for their unconditional love and encouragement throughout my degree. Your support has been integral to my success.

TABLE OF CONTENTS

Chapter 1: Introduction

Chapter 2: Materials and Methods

Chapter 3: Results

Chapter 4: Discussion

LIST OF FIGURES

LIST OF TABLES

ABBREVIATIONS

AGO7 - ARGONAUTE7
ATAF - ARABIDOPSIS TRANSCRIPTION ACTIVATION FACTOR
AM - Arbuscular mycorrhizal
BP – Base Pair
CUC - CUP-SHAPED COTYLEDON
DH_2O – Distilled Water
DNA - Deoxyribonucleic Acid
EDTA - Ethylenediamine Tetraacetic Acid
FSTs - Flanking Sequence Tags
GOI - Gene of Interest
GS – Gene-Specific
GUS - *Escherichia coli* Beta-glucuronidase
HS- Hoagland's Solution
KOH - Potassium Hydroxide
LysM - Lysin Motif
MtGEA - *Medicago truncatula* Gene Expression Atlas
MtARF3 - AUXIN RESPONSE FACTOR3
MtNFP - *M. truncatula* Nod Factor Perception
NaCl - Sodium Chloride
NAC-TF - NAM, ATAF1/2, and CUC2 Transcription Factor
NAM - NO APICAL MERISTEM
PALM1 - PALMATE-LIKE PENTAFOLIATA1
PCR - Polymerase Chain Reaction
PHAN - PHANTASTICA
qPCR - Quantitative Polymerase Chain Reaction
SA – Salicylic Acid
SDS - Sodium Dodecyl Sulfate
SGL1 - LEAFY/ UNIFOLIATA orthologue SINGLE LEAFLET1
Tnt1 F2 - Tnt1 Forward Primer
Tnt1 R2 – Tnt1 Reverse Primer
TRIS - Tris(hydroxymethyl)aminomethane
WGA - Wheat Germ Agglutinin
WPP – Weeks Post Planting
Xg - Relative Centrifugal Force

CHAPTER ONE

Introduction

1.1 Introduction

The symbiotic associations between Arbuscular mycorrhizal (AM) fungi and plant roots are ancient and ubiquitous across the plant kingdom, where up to 80% of terrestrial angiosperm species are involved in said mutualism (Brundrett, et al., 1996; Harrison, 2005). AM fungi enhance the growth of many economically relevant plant species, including food crops such as carrots, potatoes, tomatoes, peppers, and lettuce (Bagyaraj, Sharma, and Maiti 2015; Gianinazzi-pearson 1996). By definition, both partners in a mutualistic association must benefit; acting as an auxiliary root system, AM fungi provide phosphorus, water, and other minerals from the surrounding environment that the host plant is unable to access, and in turn the fungus receives photosynthetically fixed carbon in the form of lipids and sugars (Koide & Elliott, 1989; Jiang et al., 2017; Maclean et al., 2017; Bravo et al., 2017). A host plant may receive 70–100% of its Phosphorus intake from the mutualism shared with AM fungi, while the fungi sequester up to 20% of the host plant's carbon (Bago et al., 2002; Jiang et al., 2017). In addition to increased nutrient acquisition, AM fungi are associated with increased plant resistance to both abiotic and biotic stressors such as drought and plant viruses by increasing root surface area and inducing host plant resistance, respectively (Begum et al., 2019). Although considered to be a beneficial symbiotic relationship, host plants only engage with AM fungi when growing in nutrient-limiting conditions, and host plants tightly regulate AM fungal colonization to prevent the symbiont from imposing too great of a metabolic load (Gutjahr & Parniske, 2017).

Fossil records of symbiotic structures inside the roots of the Devonian land plant, *Aglaophyton major* suggest the association of these symbionts to span upwards of 400 million years (Remy et al., 1994). It is hypothesized that AM fungi enabled plants' transition from aquatic to terrestrial environments through facilitating the acquisition of vital nutrients and increasing physical stability in soil dominant habitats (Rich et al., 2021). The importance this relationship has had in shaping our past and current ecosystems cannot be understated. Despite the long-existing evidence for the co-evolution of plants and AM fungal across the world (Paszkowski 2006; Pirozynski and Malloch 1975), there is currently limited knowledge about which host genes are involved in controlling and regulating the association (Remy et al., 1994; Redecker, et al., 2000; Bravo et al., 2016). To date, most genes discovered to be involved with AM fungi symbiosis were identified through commonalities shared with *Rhizobium* legume symbiosis, and through reverse genetic analyses (Parniske et al., 2008; Gutjahr et al., 2013). By understanding the underlying genetic mechanisms involved in AM symbioses, plant growth could potentially be enhanced while reducing the need for phosphorus-rich chemical fertilizers (Berruti et al., 2015). To identify potential host genes associated with AM symbiosis, we propose a reverse genetic study of two mutant *Medicago truncatula* (*M. truncatula*) genes selected from the *Tnt1* Mutant Database at the Noble Research Institute (Tadege et al., 2008).

1.2 Fertilizer Use in Agriculture

The nutrients most limiting to the development of crop plant growth include the elements nitrogen and phosphorus (Conley et al., 2009). To enrich nutrient-depleted soils and ensure maximal crop yield and quality, farmers commonly apply commercial fertilizers containing phosphorus and nitrogen. However, crops only absorb a small percentage of the applied nutrients, and most of the nitrogen and phosphorus either runs off into the surrounding environment or becomes insoluble and inaccessible to the plants (Beman et al., 2005; Vance et al., 2003). Fertilizer runoff has become a longstanding issue around the world, where aquatic ecosystems such as freshwater lakes and streams become subject to eutrophication. Eutrophication is a phenomenon where bodies of water become contaminated with large quantities of nitrogen and phosphorus to the point where populations of cyanobacteria explode, or “bloom” (Beman, Arrigo, and Matson 2005; Fried, Mackie, & Nothwehr 2003). These blooms result in decreased dissolved oxygen concentration, increased toxin levels, and a largely reduced water quality (Conley et al., 2009). As marine environments are not closed ecosystems, the surrounding life (including humans, pets, and economically important wildlife) can face severe consequences including illness and death (Codd et al., 2006). There are also concerns about raw phosphate rock (PRock) shortages (one of the main components of commercial fertilizer) as the global demand for food skyrockets (Li et al. 2017). Therefore, there is a significant push to identify more sustainable and less damaging alternatives to the commercial fertilizers currently used by many farmers (Roy-bolduc and Hijri 2011).

A promising alternative to commercial fertilizers that have been in use for decades includes using AM fungi as a “biofertilizer” (Borde, 2009; Berruti et al., 2015; Menge 1983; Ndung et al. 2013). Through this method, AM fungi are added to crop fields to exploit the nutrient transfer that occurs during mycorrhizal symbiosis. Because AM fungi are a regenerative source, and because these microbes help plants uptake nutrients that already exist in the soil, AM symbiosis mitigates many of the concerns associated with the global overuse of commercial fertilizers.

The effectiveness of AM fungi as a biofertilizer is currently debated, and studies have exemplified inconsistent results, ranging from little/no effect on growth to a significant effect on increasing growth (Carpio, Davies, and Arnold 1962; Cozzolino, Meo, and Piccolo 2013; Kokkoris et al. 2019). To increase the effectiveness of AM symbiosis, and to decrease the use of commercial fertilizers without a loss of crop yield, it is vital that we further investigate the role of host plant genes in regulating AM fungal symbiosis.

1.3 Arbuscular Mycorrhizal Fungi

Arbuscular mycorrhizal (AM) fungi comprise over 334 known species of soil-borne fungi from the class *Zygomycotina*, order *Glomales* (Schüßler, 2017). As obligate endosymbionts, fungal propagation is only possible through association with intact plant roots in nature and greenhouses or excised root cultures in a lab (Schüßler et al., 2017). These fungi cannot fix carbon and require a host to complete their life cycle through the provision of plant-derived carbon (Lanfranco et al., 2016; Roth & Paszkowski, 2017). AM fungi are generally considered to not have a high degree of host specificity and can form associations with many different species (Sanders, 2003).

Characterized as endomycorrhizae, the primary structure of AM fungi is formed inside plant root cells. If a dormant spore in soil perceives signalling hormones from a host plant, the spore germinates to form a hyphal tube that grows towards the host plant (Seddas et al., 2009). A hyphopodium then forms on the root surface, and fungal mycelium colonizes plants' inner cortical root cells to form storage vesicles in many species, and tree-like structures called arbuscules- the primary site of nutrient exchange (Seddas et al., 2009).

AM fungi acquire phosphorus from the rhizosphere in two ways. The first mechanism may be attributed in part to AM fungal hyphae, which may establish mycelial networks kilometres in length, considerably beyond the length of any host plant's roots. The extensive hyphal network effectively increases fungal surface area in the soil to allow for increased contact with nutrients that plant roots could not otherwise reach. In addition, AM fungi have been shown to form a mutualistic association with phosphatase secreting bacteria, which provides another source of soluble phosphorus to the fungi that a host plant may not access on its own (Wang et al., 2017; Ezawa & Saito, 2018; Sato et al., 2019). A vital macronutrient for plants, nitrogen is a crucial component of amino acids, which serve as the building blocks for enzymes and proteins in plants (Leghari et al., 2016). AM fungi acquire nitrogen through hyphal absorption of decomposing organic sources (Leigh et al., 2009).

Considered a keystone species, AM fungi shape the world around us. These microscopic fungi inhabit a broad range of habitats, spanning arctic regions, tropical forests, and deserts (Basu et al. 2018; Chen et al. 2018; Cosme et al. 2018; Bonfante and Venice 2020). Research indicates that AM fungi both offer structure to the soil and reallocate nutrients in ways that sustain the stability of ecosystems (Walder, 2015; Chen et al. 2018; Whiteside et al. 2019). Studies indicate that AM fungi can sequester heavy metals away from host plants through hyphal absorption and adsorption, effectively immobilizing metals in the mycorrhizosphere (Joner et al., 2000; Christie et al., 2004; Bhargava et al., 2012). Frequently used in agriculture, AM fungi are observed to increase crop yields and decrease fertilizer needs for many economically important plant species (Zhang et al., 2019).

Rhizophagus irregularis (*R. irregularis*), formerly *Glomus intraradices*, is the most studied species of AM fungi today (Parniske 2008; Rosikiewicz, 2017), and comprise the most popular inoculum for commercial mass-production (Berruti et al. 2016). *R. irregularis* has become the most popular species in research for a reason: they colonize host plants quickly by generating many daughter spores and forming large hyphal networks, and they grow rapidly in *in vitro* conditions (Berruti et al. 2016). In addition, the complete genomic sequence of a *R. irregularis* strain was made available in 2013, and more than 10 strains are sequenced in their entirety today (MycoCosm: The Fungal Genomics Resource, 2020). The species of AM fungi used in the research of this thesis is *R. irregularis*.

Many aspects of AM fungal biology are poorly understood; they remain a difficult subject for molecular investigation because they are multinucleated, obligate symbionts (Schüßler et al., 2017). Their modes of reproduction and mechanisms of nuclear exchange remain elusive. Despite rapid advances in genetic technology, little information exists regarding the establishment of methods to genetically transform AM fungi. Prospective transformation is further complicated by our inability to produce protoplasts from these fungi (Harrier and Millam, 2001). Therefore, current knowledge regarding the symbiotic machinery that supports plant-AM symbiosis is skewed toward the plant host.

1.4 Colonization by Arbuscular Mycorrhizal Fungi

The association shared between AM fungi and host plants follow a stepwise process with distinct stages. The outcome of the symbiosis is dependent on molecular communication that arises prior to physical contact between the partners (Seddas et al., 2009; Harrison, 2005). The symbiote's dialogue begins when signalling molecules are exchanged between the host plant's roots and AM fungal spores within the rhizosphere, a narrow region of topsoil where root secretions are produced (Padje & Kiers, 2016; Choi et al., 2018). Plant roots signal with strigolactone, which AM fungi detect and respond by growing towards (Padje & Kiers, 2016). Research indicates that plant roots release greater concentrations of strigolactones when they are deficient in phosphorus (López-Ráez et al., 2011), which effectively signals AM fungi for colonization (Padje & Kiers, 2016).

In parallel, AM fungi secrete mycorrhizal factors (Myc factors), lipochito oligosaccharides and chitin, which activates the plant's common symbiosis signalling pathway (SYM pathway) and induces increased growth and branching in host roots (Maclean et al. 2017; Basu et al. 2018; Chen et al. 2018; Cosme et al. 2018). CERK1, a lysin motif (LysM) pattern recognition receptor is mobilized for symbiotic signaling in the presence of mycorrhizal fungi, and activates the SYM pathway (Feng et al., 2019; Miyata et al., 2014). DMI1, DMI2, and DMI3 are additional common SYM pathway genes integral to detecting Myc factors (Genre et al., 2013). These genes are also involved in inducing a nuclear calcium spike that prompts the signalling of genes required for symbiosis (Oldroyd & Downie, 2006).

Upon contact between AM fungal hypha and a host plant, the host plant gene expression of defence-related hormones that are typically elicited when encountering outside microbes becomes suppressed (García-Garrido & Ocampo, 2002). For example, salicylic acid (SA), a phytohormone which plays a role in defence responses against biotrophs is downregulated upon contact with AM fungal hyphae (Kapulniki et al., 1996). It is unknown whether host plants recognize AM fungi as beneficial, and consequently downregulate their innate defence response, or if AM fungi have a mechanism to override plant host defence responses- or perhaps a combination of both (Kloppholz et al., 2011).

Once reciprocal recognition has occurred, important cellular changes transpire to allow for colonization by AM fungi. The host plant's nucleus first moves towards the point of contact with the fungus, and the central vacuole is fragmented (Genre and Bonfante, 2005). The fungus produces a hyphopodium upon the host's root epidermal cells, and a host pre-penetration apparatus guides the hyphae into the apoplastic space between cells. The hyphopodia then penetrate the plant root epidermal cells to initiate infection (Choi et al., 2018; Siciliano et al., 2007). The plant's inner cortical cells reorganize to allow formation of arbuscules, highly branched "tree-like" structures (**Figure 1.1**), which become the primary interface of nutrient exchange between the organisms (Choi et al., 2018). The periarbuscular membrane, derived from the plant host, surrounds the arbuscules and includes transporters that transfer nutrients throughout the symbiotic association (Breuillin-Sessoms et al., 2015; Javot, Pumplin, et al., 2007; Krajinski et al., 2014). Arbuscules persist for seven to 10 days before degrading, at which point the host plant root cortical cells return to their pre-colonization state, and may be re-colonized (Pumplin & Harrison, 2009).

Once the symbiosis has been established, host plants retain a high degree of control over the extent of fungal colonization and continuation of the mutualism (Gutjahr & Parniske, 2017). Host plants can detect the level of nutrients being transferred by the AM fungi and adjust the quantity of carbon conveyed in return (Ji & Bever, 2016; Grman, 2012; Kiers et al., 2011). Research indicates that sections of roots receiving lower quantities of phosphorus and other nutrients acquired through the mutualism will subsequently provide lower amounts of carbon to the fungi in return (Ji & Bever, 2016). These checks and balances allow for the host plant to avoid being exploited of carbon and keep the association mutualistic.

1.5 The Module Legume *Medicago truncatula*

M. truncatula is a model species for genomic investigations because of its small diploid genome (390 Mbp), quick generation time, autogamy, and high transformation efficiency (Trieu et al., 2000; Cook, 1999; Barker et al., 1990). It is closely related to alfalfa (*Medicago sativa*), an important fodder legume, and can serve as a model species for other economically important legumes, such as soybean (*Glycine soja*). *M. truncatula* engages in symbioses with nitrogen-fixing *Rhizobium* and AM fungi, unlike *Arabidopsis thaliana*, the most commonly studied genetic model plant. Due to genetic overlap between *Rhizobium*-legume and AM fungi-legume symbiosis, *Rhizobium*-legume associations have been used to uncover genes associated with AM symbiosis (Kistner & Parniske, 2002).

Online resources for *M. truncatula* are abundant. The *Medicago truncatula* Gene Expression Atlas (MtGEA) is an expansive database created by GeneChip analysis; with gene expression data from over 156 Medicago genome arrays, the database is integral for analyses of the *Medicago* transcriptome (He et al, 2009). This resource is used to identify genes that are expressed in tissues of interest, and to assess the expression of genes of interest under various conditions (Benedito et al., 2008). This software facilitated the identification of genes that may be involved in AM fungal root colonization and was used by Dr. Allyson MacLean to identify the two genes examined in this thesis.

1.6 *Medicago Tnt1* Mutant Library and Mutant Lines of Interest to this Study

The Noble Research Institute *Tnt1* Mutant Database has created over 16,000 *Tnt1* mutant lines with an average of 25 *Tnt1* insertions per line in the *M. truncatula* R108 ecotype genome (Noble Research Institute, 2013). Each *Tnt1* insertion is around 5.3 kb (Cheng et al., 2011). Flanking sequence tags (FST) are utilized for identifying the location of said insertions and are BLAST-searchable (Cheng et al., 2011).

The mutant lines were created using insertional transposon mutagenesis, a method used to produce loss-of-function mutants, whose resulting phenotypes assist in determining a gene's function (Alonso et al., 2003). *Tnt1*, the long terminal repeat (LTR) retrotransposon of tobacco (*Nicotiana tabacum*), frequently utilized in reverse genetic studies, was used to tag the mutant plant populations (Alonso et al., 2003, Noble Research Institute, 2013).

Tnt1 insertions are considered to be stable throughout a plant's life cycle (Cheng et al., 2011). Accordingly, *Tnt1* insertions segregate for the mutation and may be inherited in both alleles, one allele or neither allele, creating a genotype of *Tnt1* homozygous, heterozygous or wildtype (WT) homozygous, respectively (**Figure 1.2**). The experiments produced in this thesis use WT homozygous plants as a control in addition to R108 WT plants because (unlike R108) WT homozygous plants share all the same *Tnt1* insertions as the homozygous mutant plants- except for the insertion truncating the gene of interest (Cheng et al., 2011).

1.6.1 NAC Transcription Factor like (NAC TF)

The NAC TF gene belongs to one of the largest families (152 in soybean) of plant-specific transcription factors (Le et al., 2011). The first known NAC protein identified was NO APICAL MERISTEM (NAM) in petunia, then ARABIDOPSIS TRANSCRIPTION ACTIVATION FACTOR (ATAF) and CUP-SHAPED COTYLEDON (CUC), discovered in Arabidopsis (Tran et al., 2004; Zhong et al., 2006). Other plant species, including rice, wheat, and soybean, have been shown to encode NAC proteins (Hussey et al., 2015).

The NAC TF family is characterized by a highly conserved 150-amino-acid NAC domain that includes five subdomains (A–E) at the N-terminus ends and a highly variable domain at the C-terminus ends (Ernst et al., 2004). NAC TFs are also sometimes comprised of alpha-helical transmembrane motifs (TMs) at their C-terminal end (Puranik et al., 2012).

NAC proteins regulate plant development, improve mineral absorption, and increase crop nutrition and quality. NAC TFs have a role in regulating a range of physiological processes in plants, including auxin transport and cell death (Yoshii et al. 2010). When plants are exposed to biotic or abiotic stress, NAC TFs engage in several signalling pathways to help them mitigate the stress (Pinheiro et al. 2009).

Despite the functional characterization of NAC proteins in many plant species, little research has investigated their function in *M. truncatula*. Zélicourt et al. (2011) reported that *MtNAC969*, a NAC TF gene up-regulated by salt stress (Gruber et al., 2009), affects *M. truncatula* root morphology and symbiotic nodulation. RNAi-mediated silencing of *MtNAC969* stimulated the formation of lateral roots, and overexpression of *MtNAC969* resulted in the production of a shorter and less branched root system. These findings indicate that the NAC TF is implicated in several pathways necessary for adaptive root responses to salt stress and the formation of a functioning symbiotic nodule (Gruber et al., 2009). Ling et al., (2017) demonstrated that gene members of the NAC family are expressed under diverse abiotic stresses such as cold, salinity, and drought in *M. truncatula*, using expression profiling and RNA-seq data analysis.

Based on expression data from the *Medicago truncatula* Gene Expression Atlas, Dr. Allyson MacLean identified a gene encoding NAC TF that was expressed in *M. truncatula* roots infected with *R. irregularis* but not in the uninoculated control. Considering the role of these genes in symbiotic associations and stress responses, we tested the potential involvement of this gene by measuring the mean root length colonization of a homozygous *Tnt1* mutant when inoculated with AM fungi.

1.6.2 Palmate-like Pentafoliata (*PALM1*)

PALM1 encodes a transcription factor with a single Cys(2) His(2) zinc finger DNA binding domain at the N-terminus and an EAR transcription repressor domain at the C-terminus *(*Chen et al., 2010). *PALM1* is known to play a role in the maintenance and regulation of the dissected trifoliate leaf structure of mature WT *M. truncatula* plants *(*Chen et al., 2010). In *Medicago truncatula*, *PALM1* is a crucial regulator of compound leaf patterning. SGL1, a critical regulator of lateral leaflet initiation, is negatively regulated by *PALM1* (Peng et al., 2017). Loss-of-function mutants of *PALM1* displayed a phenotype of palmate-like pentafoliate leaves (two additional leaflets per leaf when compared to the Wildtype control), and increased petiole length increased by ~20% compared with WT *M. truncatula* (Chen et al., 2010; Ge at al., 2014).

PALM1 transcripts are expressed in vegetative shoot buds, leaves, and developing seeds, but gene expression is absent or hardly detectable in roots, petioles, stems, flowers, pods, and seed coats, according to in silico microarray-based expression analyses (Chen et al. 2010).

It has been demonstrated that *PALM1* suppresses the expression of the LEAFY/ UNIFOLIATA orthologue SINGLE LEAFLET1 (*SGL1*), which encodes an indeterminacy factor required for leaflet initiation in *M. truncatula* (Chen et al., 2010). *PALM1* mutant transcriptome analysis by Uppalapati et al., (2012) indicated that *PALM1* downregulates *eceriferum4*, an enzyme involved in primary alcohol biosynthesis, and *MYB96*, encoding a key transcription factor that controls wax biosynthesis. These results demonstrate that *PALM1* regulates epicuticular wax metabolism and transport, and epicuticular wax modulates rust spore differentiation of host and nonhost fungal pathogens (Uppalapati et al., 2012).

Peng et al. (2017) discovered a mechanism for the regulation of *PALM1*, where *M. truncatula* AUXIN RESPONSE FACTOR3 (*MtARF3*) functions as a direct transcriptional repressor of *PALM1*. Upregulation of *MtARF3* or removal of both PHANTASTICA (*PHAN*) and ARGONAUTE7 (*AGO7*) pathways resulted in the palmate-like five-leaflet leaf structure in *M. truncatula (*Peng et al., 2017).

Based on expression data from the *Medicago truncatula* Gene Expression Atlas, Dr. Allyson MacLean identified a gene encoding *PALM1* that was expressed in *M. truncatula* roots infected with *R. irregularis* but not in the uninoculated control. In addition, considering the role of *PALM1* in the morphological development and recognition of fungal pathogens in *M. truncatula*, we were motivated to study the involvement of this gene in regulating AM symbiosis.

1.7 Research justification and objectives

Using Affymetrix Gene Chip data from the *Medicago truncatula* Gene Expression Atlas and RNAseq data of colonized *M. truncatula* roots (MacLean & Harrison, unpublished data), we identified two host genes that exhibit increased expression exclusively during AM fungal events (**Table 1.1**). These expression profiles suggest the genes' involvement in mediating root colonization and/or arbuscular development. This study will apply a reverse genetics analysis to these two *M. truncatula* genes to determine their role in establishing and/or supporting AM symbiosis.

The main goal of my research is to assess the involvement of two *M. truncatula* genes in mediating AM symbiosis, specifically by observing the interactions between the host plant and fungi through the measurement of root colonization and arbuscular development. If the genes under study have a role in mediating AM fungal symbioses prior to and/or during root infection, we hypothesize that we will observe a difference between the colonization rates of the mutant and control groups.

The greater purpose of this study is not only to better understand the biology of *M. truncatula* association with AM fungi but also to pursue more effective ways to adopt AM fungi symbiosis in sustainable agroecosystems. As the current overuse of chemical fertilizers has caused devastating consequences to the environment (Berruti et al., 2015), the practical applications of this research remain promising.

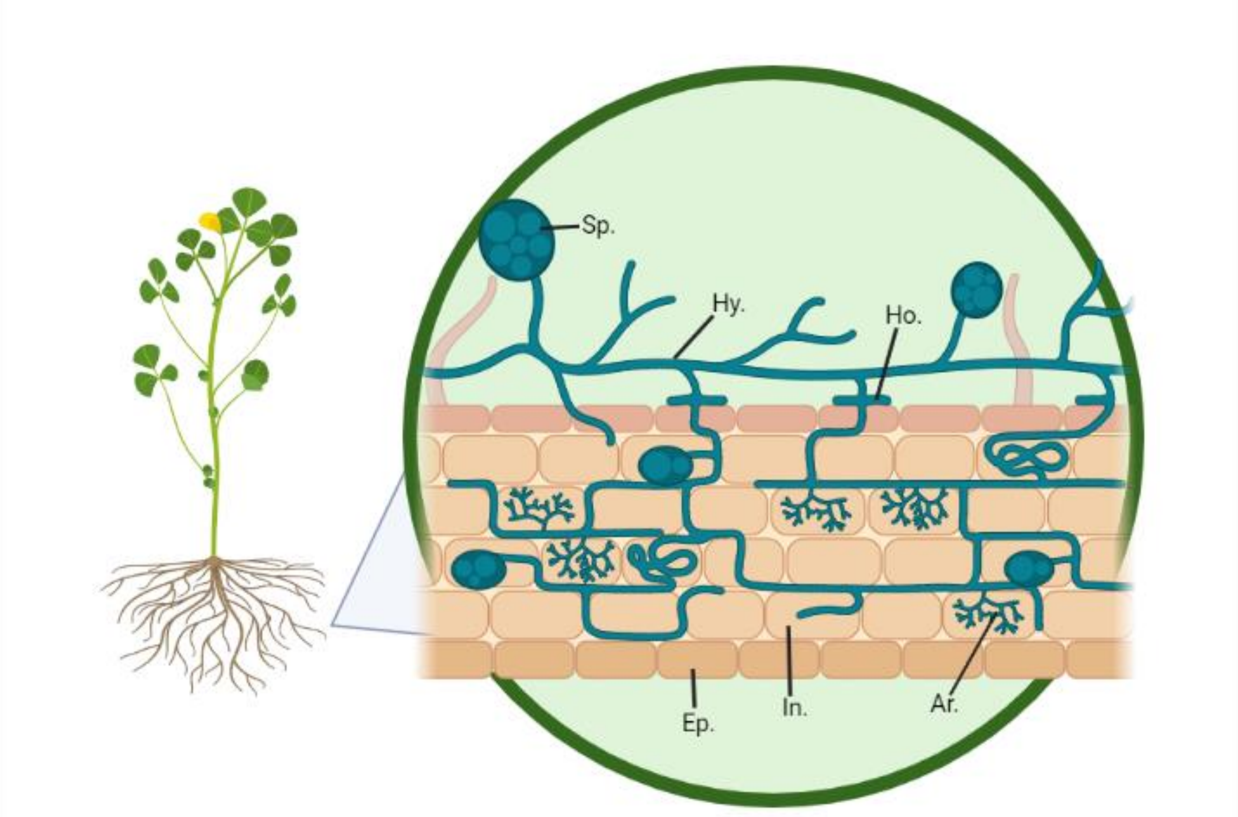

Figure 1.1 Colonization of host plant roots by arbuscular mycorrhizal fungi. AM fungi germinate to form hyphae that grow towards the host plant. The hyphopodium then penetrates host plant root cells, and mycelium colonizes plants' inner cortical root cells to form storage vesicles, and tree-like structures called arbuscules. Ar: Arbuscule, Ep: Epidermal cells, In: Inner cortical cells, Ho: Hyphopodium, Hy: Hyphae & Sp: Spores.

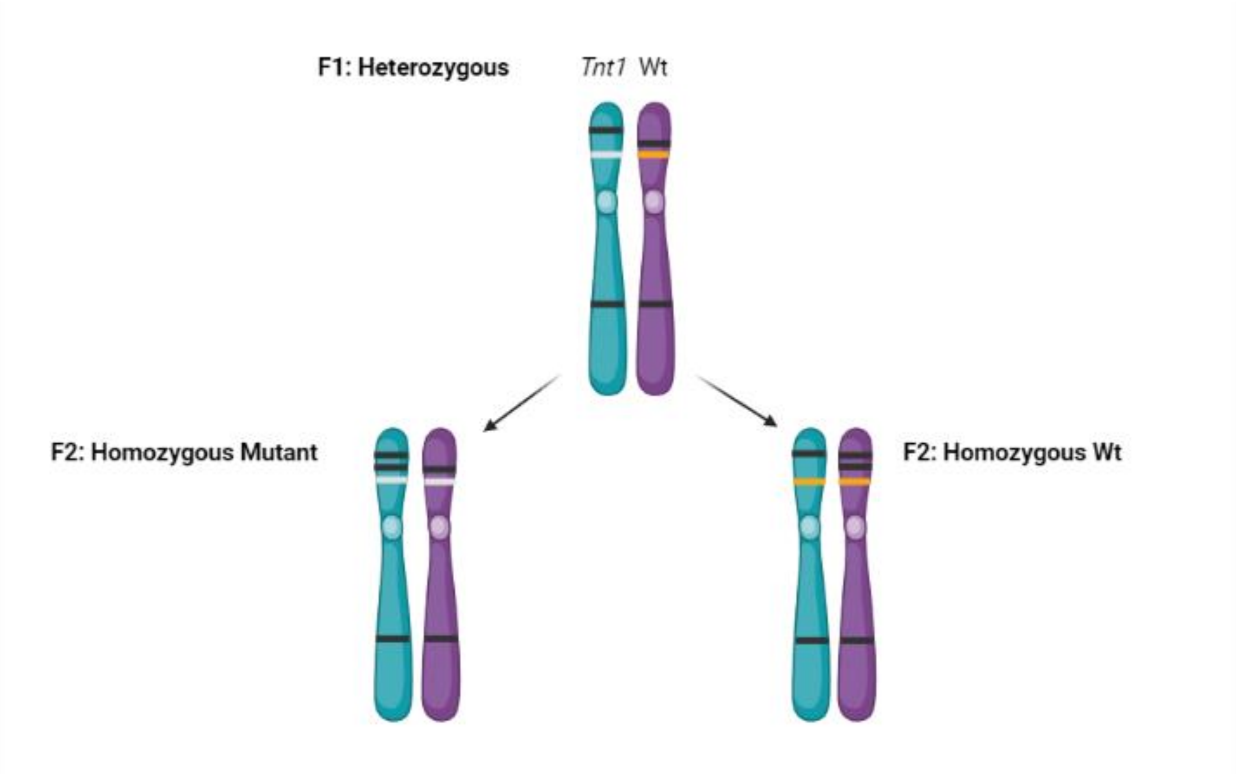

Figure 1.2. The segregation of a Tnt1 transposon from heterozygous parent plants to homozygous offspring in self-fertilizing *Medicago truncatula* obtained from the Noble Foundation. White lines depict the gene of interest being truncated by a Tnt1 retrotransposon. Orange lines depict a wild-type copy of the gene of interest. Black lines depict the location of background insertions in non-relevant genes.

Table 1.1. Two *M. truncatula* genes with increased expression during AM fungal symbiosis. Each gene has at least one *Tnt1* insertion in one exon. Plant lines were acquired from the Noble Foundation

Gene ID	**Gene product**	**Function**	**Mutant lines**	***Tnt1* location**	**Gene size (BP)**
Medtr7g100990	NAC transcription factor-like protein (NAC TF)	Involved in the secretion of defence hormones	NF18398	Exon 1	1,777
Medtr5g014400	Palmate-like Pentafoliata (*PALM1*)	Regulation of the trifoliate leaf structure of *M. truncatula*	NF18424	Exon 1	756

CHAPTER TWO

Materials and Methods

2.1 *Tnt1* mutants

We obtained 10-15 seeds for two *M. truncatula Tnt1* mutant lines (*Medtr7g100990* & *Medtr5g014400*) from the Noble Research Institute *Tnt1* Mutant Database (Tadege et al., 2008). To acquire an adequate number of seeds (>100) for symbiosis experiments, the *Tnt1* seeds were sterilized and grown in a greenhouse in pots mixed with equal parts sand, Turface. The plants were fertilized twice weekly with 20 mL Hoagland's solution (HS) and watered on alternate days. Seeds were harvested once mature.

2.1.1. DNA extraction

One-three mature leaves from each plant were randomly selected for DNA extraction following the protocol as described by Sika et al (2015). Leaves were collected from an *M. truncatula* experimental plant, flash-frozen using liquid Nitrogen and crushed with a plastic pestle inside a 1.5 mL centrifuge tube until becoming a fine powder. Then, 400 uL of DNA extraction buffer (0.2M TRIS (pH 8), 0.25M NaCl, 0.025M EDTA, 0.05% SDS) was added to the centrifuge tube with the crushed samples and vortexed to mix. The samples were centrifuged at 12,000 xg for seven minutes. The supernatant was removed, and 400 uL of isopropanol was added to the supernatant to precipitate DNA, and the sample was then centrifuged at 12,000 xg for ten minutes. Keeping the pellet intact, the supernatant was removed and 500 uL of 70% ethanol was pipetted into the centrifuge tube to wash the pellet. The samples were then centrifuged at 12,000 xg for ten minutes. The ethanol was carefully removed, and the pelleted DNA was left to dry in a flow hood for one minute before pipetting 50 uL of DH_2O to dissolve the pellet. The samples were kept at -20°C for medium-term storage and -80°C for long-term storage.

2.1.2. Genotyping

A subset of *M. truncatula* experimental plants was genotyped to ensure the inclusion of the *Tnt1* insertion in the gene of interest and to confirm the zygosity of the plants at the insertion site (Possible genotypes: *Tnt1* homozygous, heterozygous, or Wild Type homozygous) (Cheng et al., 2011).

2.1.2.1. Primer design

Flanking sequence tags (FSTs) (about 300 bp) corresponding to where a *Tnt1* transposon has integrated are provided via the Noble Foundation Genetic Genome Browser (Tadege et al., 2008). The *M. truncatula* genome sequence (A17 ecotype) can be acquired through NCBI and was used to create gene-specific (GS) primers that flank either side of the expected integration site in *M. truncatula*. The total amplicon size of the gene in the absence of the insertion was between 500 and 700 bp (**Table 2.1**). Cheng et al. provided the Tnt1 forward (Tnt1 F2) and reverse primer (Tnt1 R2) sequences (**Table 2.1**) (2011).

2.1.2.2 Polymerase chain reaction (PCR)

The GoTaq DNA polymerase was used to perform the PCR (Promega Corporation, 2002), following the manufacturer’s protocol. To visualize, PCR products were run on a 0.8% agarose gel at 100 volts. Redsafe staining and UV light were used to visualize the gels. To ascertain the genotype of each plant of interest, two PCRs were used to amplify the extracted DNA using both *Tnt1* forward and reverse primers, and gene-specific primers that were previously created using NCBI's A17 genome database (**Table 2.1**)

2.1.2.3. PCR interpretation

As the orientation of the inserted transposon was unknown, the first PCR on each mutant line was accomplished by Co-op student Dominique Daniels with four alternative primer combinations: 1) GS F + Tnt1 F2, 2) GS F + Tnt1 R2, 3) GS R + Tnt1 R2, 4) GS R + Tnt1 F2 (Cheng et al., 2011). Because only two of the four primer combinations yielded results, this first PCR offered information on the direction of the insertion (**Figure 2.1**). Based on the quality of the amplified product formed on the gel, one of the primer combinations was selected for continued genotyping. This primer set assisted in determining whether the insertion was present but did not indicate the insertion's zygosity. With an amplified product of the correct size present, the plant was either homozygous for the *Tnt1* insertion, where both copies of the gene were truncated or heterozygous for the *Tnt1* insertion. If there was no amplified product, the plant was most likely homozygous for WT at the insertion location. The proper gene-specific (GS) forward and reverse primers were used to run PCR on each plant to indicate whether the *Tnt1* insertion was homozygous.

Plants which were homozygous for the gene of interest (GOI) were named "*Tnt1* homozygous", while plants with segregating background insertions while homozygous WT at the GOI were named "segregating WT".

2.1.3. Tnt1 insertion sequencing

The Noble Foundation *Tnt1* mutant database provides flanking sequence tags (300 bp) in which the *Tnt1* transposon is believed to have integrated into each of the mutant lines, but it is critical to confirm the exact location of the insertion, and that the transposon is integrated into an exon to confirm that it is not spliced out with the introns.

PCR products generated using the appropriate *Tnt1* and GS primers (**Table 2.1**) were sent to GenomeQuebec for Sanger sequencing to establish the exact position of the *Tnt1* insertion. This process was completed by Co-op student Dominique Daniels.

2.2 Symbiosis assays

To periodically detect any phenotypes that may be expressed at different stages of the mutualism, each treatment within the symbiosis assays consisted of 8-9 replicates for each control and mutant treatment groups, sampled at two-three timepoints of varying weeks (Montero et al., 2019). Symbiosis assays were conducted using Cone-tainers (2 cm radius and 21 cm length), cylindrical shaped cones that save space within the limited space of a growth chamber. Two plants of the same genotype were planted in each Cone-tainer.

2.2.1 Seed sterilization

To limit the risk of microbial contamination that may interfere with AM symbiosis, *M. truncatula* seeds were sterilised before planting. The desired quantity of *M. truncatula* seeds were extracted from their seed pods and immersed in concentrated sulfuric acid for nine minutes to remove the hydrophobic seed coat. The seeds were then rinsed five times in dH_2O. To sterilise the seeds, a 10% bleach and 0.1% Tween 20 solution was applied to the seeds which were shaken for 10 minutes. The seeds were then rinsed 5 times with sterile dH_2O in a flow hood. To avoid proximity inhibited germination, the seeds were then spaced apart on moist filter paper in a petri dish. To break dormancy and facilitate synchronised germination, the petri dish was kept at 4°C for at least 3 days. The petri plates were then kept in a dark drawer overnight to germinate at room temperature. Following, the plates were placed in front of a bright window for two days to allow the cotyledons to grow. The seedlings were then ready for planting.

2.2.2 Cone-tainer preparation

Cone-tainer's were soaked in a 10% bleach solution for ten minutes before being sprayed with 70% ethanol. One-inch marbles were then placed inside each Cone-tainer. The marble was covered with an inch of Turface, then three inches of autoclaved sand and Turface in a 1:1 mix. The surface of this mixture was then covered with 200 spores (0.250 g) of MYKE® PRO WP (Premier Tech) brand *R. irregularis*. A two-inch layer of autoclaved sand and Turface mix was then used to cover the spores and fill up the rest of the Cone-tainers. Two sterilized seedlings were then planted inside the prepared cones (**Figure 2.2**). The plants were fertilized with 20 mL of half-strength (0.5x) Hoagland's solution (HS) with 20 µM potassium phosphate (Hoagland and Arnon, 1950) twice weekly. Fertilizer solutions with decreased Nitrogen and Phosphorus concentrations are associated with increased rates of AM fungal symbiosis (Douds and Schenck, 1990). Growth chamber conditions will consist of 16h light/8h dark photoperiods, held at 25°C. These conditions reflect optimal parameters of growth for both AM fungi and *M. truncatula* (Heinemeyer and Fitter, 2004).

2.2.3 Symbiosis assay harvesting

To quantify colonization rates and observe arbuscule development, the experimental *M. truncatula* roots were cleared and stained upon harvest. The harvested roots were separated from the stem, washed in water, and put in 50 mL falcon tubes. The roots were then soaked in a 50% ethanol solution for a minimum of 15 minutes. The ethanol was removed, and roots were placed in 20% potassium hydroxide (KOH) overnight at 65°C. KOH allows the roots to be cleared of lignin and results in increased transparency that allows ease of AM fungal visualization (Vierheilig et al., 2005). The KOH was removed, and the roots were covered with phosphate buffered saline solution and shaken for ten minutes, repeated two times. To visualize the AM fungi using microscopy, a wheat germ agglutinin (WGA), Alexa Fluor™ 488 conjugate was added to each sample (0.2 ng/mL) (Vierheilig et al., 2005). WGA is a lectin that attaches to chitin and allows for the visualization of fungal structures (Vierheilig et al., 2005) when bound to an Alexa Fluor™ (ThermoFisher Scientific, 2009). The treated and stained roots were kept at 4°C long-term, avoiding extended light exposure as the WGA conjugate is light-sensitive (ThermoFisher Scientific, 2009).

2.2.4. Mean root length colonized quantification

The grid line intersect method was used to quantify *M. truncatula* root colonization. Widely practiced, this method uses a Petri dish printed with evenly distributed grid lines to systematically calculate the percentage of colonized roots (Giovannetti & Mosse, 1980). The cleared and stained roots from the *Tnt1* mutant and WT control *M. truncatula* samples were evenly spread onto an 8 x 8 cm square petri dish with vertical and horizontal grid lines 1.4 cm apart for a total of 36 squares. The samples were systemically visualized using a Zeiss Axiozoom stereoscope, and each time a root crossed a gridline, the section was scored as either colonized or uncolonized. The percentage of colonization was determined for each replicate as follows:

Percent root length colonized = Total number of colonized root segments/(Total number of colonized root segments + total number of uncolonized root segments)*100

The mean root length colonized was averaged for each treatment group (*Tnt1* homozygous or segregating WT) at each time point. Once quantified, the mutant treatment groups were numerically compared to the WT control.

2.2.5 Statistical Analysis

To detect for statistical significance between the *M. truncatula* mutant groups and the control treatment, we used One-Way ANOVA for the treatment averages at each timepoint. If significance was detected ($p < 0.05$) in mean root length colonized, and the assumptions of normality, independence, linearity, and homoscedasticity were met, we concluded that the mutant line has an altered rate of AM colonization.

2.3 Root Phenotyping Assays

Root phenotyping assays were conducted using sterile *M. truncatula* seedlings grown in Turface. The plants were fertilized with 20 mL of half-strength (0.5x) Hoagland's solution (HS) twice weekly. Each treatment within the assays consisted of 20 replicates of segregating WT, *Tnt1* mutants and R108 control plants with one timepoint at two weeks. After harvest, recorded measurements included length of longest root, total root length, number of root tips, fresh root mass, fresh shoot mass, total fresh mass, total dry mass, dry shoot mass and dry root mass. Images of the plants were analyzed using ImageJ software for the length of longest root, total root length and the number of root tips. Samples were dried for three days in an oven before calculating total dry mass, dry shoot mass and dry root mass. The measurements listed above were then used to compare the physical features of the *Tnt1* mutant and control groups of *M. truncatula* (Segregating WT & R108 plants).

2.4 Leaf excision symbiosis assays

To determine if the two additional leaflets of the *PALM1 Tnt1* (**Figure 2.3**) mutant have an effect on symbiosis (measured through mean root length colonized) by means of increased photosynthetic surface area when compared to the control plants, we created a protocol for a symbiosis assay that included plants with one or two leaflets removed. The parameters of the assay were as previously described for the symbiosis assays, with one major adjustment. Starting at two weeks, leaflets were randomly removed by hand from the *PALM1 Tnt1* mutant plants. The number of leaflets removed depended on the treatment group. The first treatment consisted of the pentafoliate leaf structure being left intact and undisturbed. The second treatment consisted of leaves with one leaflet removed, resulting in four leaflets per leaf, to allow for an intermediate treatment group between the pentafoliate and the trifoliate leaf structure. The final treatment consisted of two leaflets being removed, giving three remaining leaflets, which resembled the anatomy of the Segregating WT and R108 *M. truncatula* plants. All removed leaflets were randomly selected. Leaf excision occurred when leaf development allowed for accurate and precise excision. Leaflet excision occurred once a day between Monday to Friday, or whenever new leaves had grown.

2.4.1 Leaf surface area measurements

We measured the surface area of two leaves per Cone-tainer for the controls and *Tnt1* mutant plants at each timepoint for a subset of the plants in the *PALM1* leaf excision symbiosis assays. The surface area of leaves was recorded using the mobile app Leafscan (Department of

Radiation Oncology, University of Michigan) and a smartphone (Model A1864 iPhone SE, Apple, Inc.). Pictures were obtained by pressing the leaves flat with a clear plastic cover on a white background. The image files were converted to area units by the reference markers provided by the software developer. The measurements obtained from the application were uploaded into excel before conducting statistical analysis using one-way ANOVA.

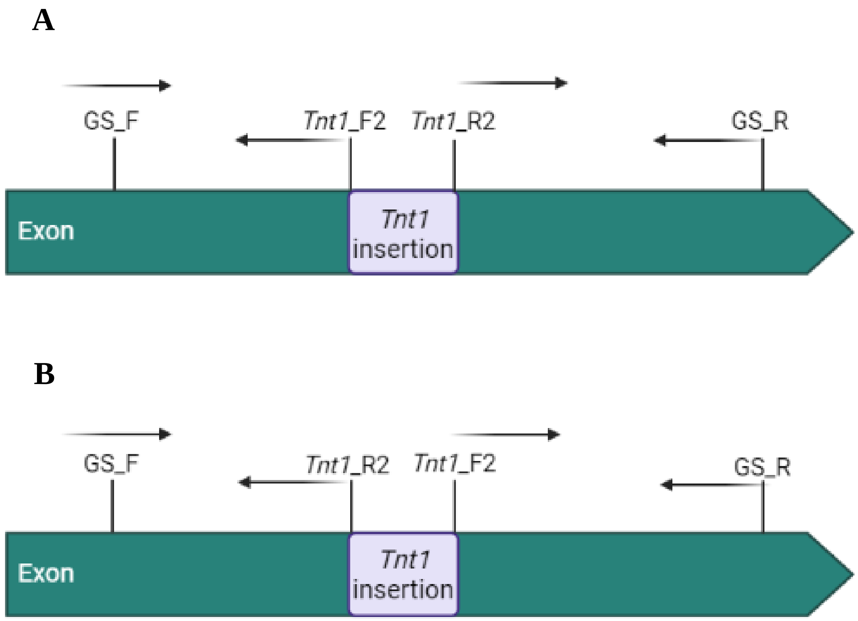

Figure 2.1. Transposon insertion in gene with primer set locations and direction. A) Two of four primer sets used for genotyping of *M. truncatula*, GS_F + Tnt1_F2, GS_R + Tnt_R2 B) Remaining two primer sets used for genotyping, GS_F + Tnt1_R2, GS_R + Tnt1_F2.

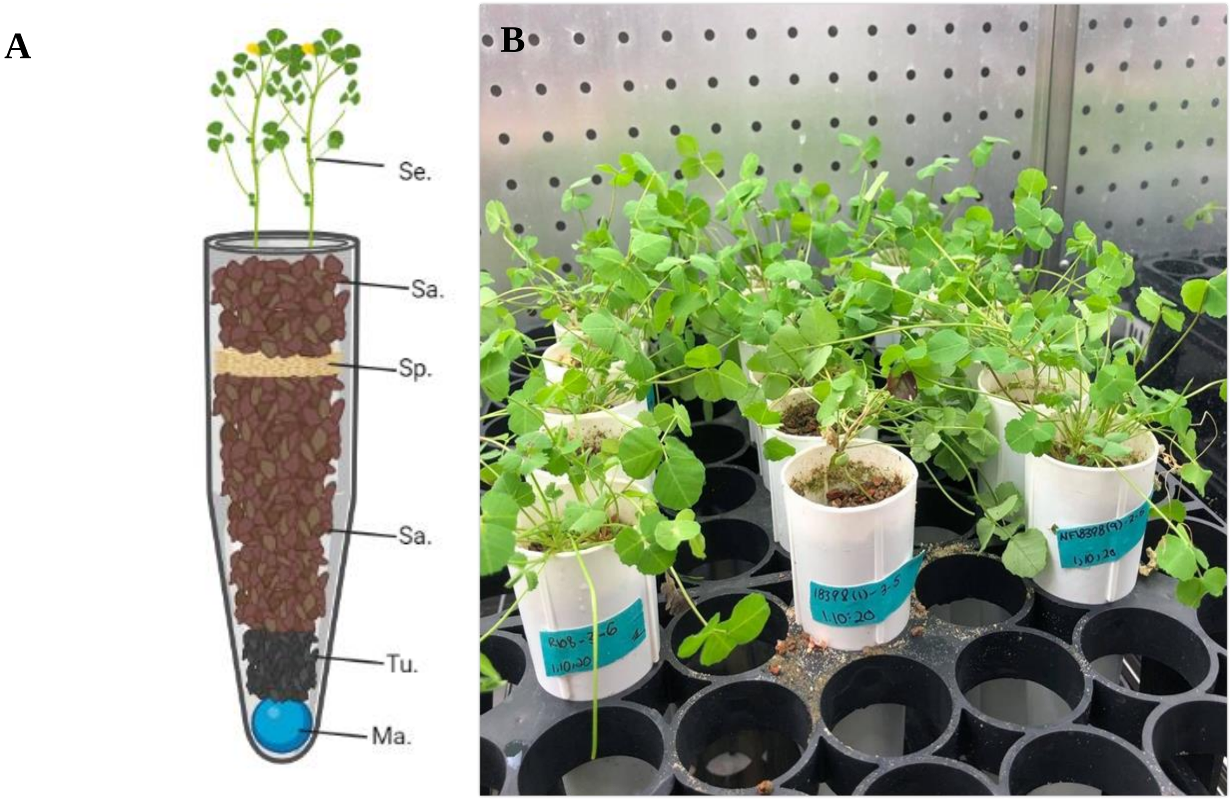

Figure 2.2 Cone-tainer preparation for Symbiosis Assays. Panel A: Representative diagram indicating how the cone-tainers are prepared. Panel B: Picture of cone-tainers after preparation. Ma: Marble, Tu: Turface, Sa: Sand and Turface mixture, Sp: Fungal Spores, Se: *M. truncatula* seedlings.

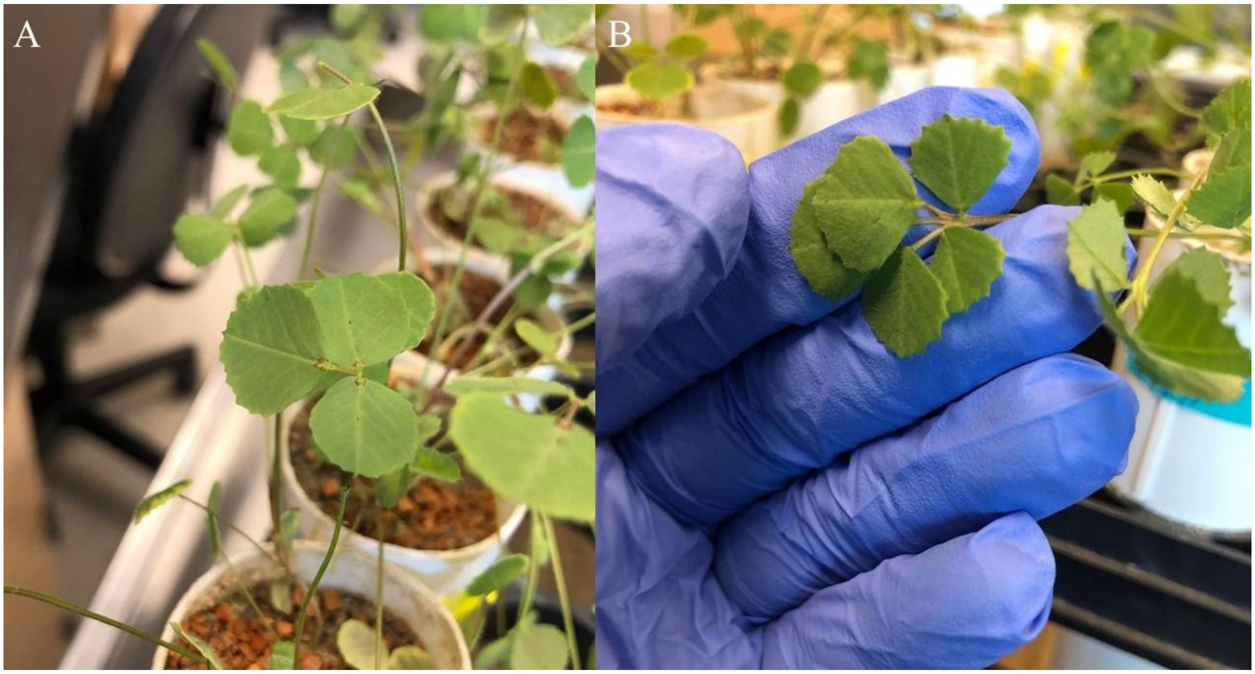

Figure 2.3 Visual Comparison of Wildtype Control and *PALM1* mutant plants. Panel A: Representative photo of Wildtype control plants with three leaflets per leaf. Panel B: Representative photo of *PALM1* mutant plants with five leaflets per leaf.

Table 2.1. Primers used for amplifying DNA from *Medicago truncatula* plant tissue

Primer name	**Description**	**Sequence (5’-3’)**
NF18398_Fw	Gene specific primers for NAC-TF gene in NF18398 mutant line	CCATTTCATATGCCCAGAGAGTCC
NF18398_Rv	Gene specific primers for NAC-TF gene in NF18398 mutant line	GCTTCCATTCCTTTAATTAACATTCCTTC
NF18424_Fw	Gene specific primers for *PALM1* gene in NF18424 mutant line	GGTAAATGGTAAAGAAGGCACAATCC
NF18424_Rv	Gene specific primers for *PALM1* gene in NF18424 mutant line	GCTACAGATATTGGCCTTCTTTCC
*Tnt1*_F2	Primers for *Tnt1* mutants corresponding to *Tnt1* insertion sites	TCTTGTTAACCGTATCTCGGTGCTACA
*Tnt1*_Rv	Primers for Tnt1 mutants corresponding to Tnt1 insertion sites	AGTTGGCTACCAATCCAAGGA

CHAPTER THREE

Results

3.1 NF mutant line sequencing data

Sequencing results of the two *Tnt1* lines showed that the location of the transposon insertion in both mutant lines (NF18398 & NF18424) is within in an exon (**Figure 3.1**). These results indicate that the proteins encoded by these genes are likely to be non-functional due to the insertion location and size (5.3 kb), which is expected to disrupt gene expression.

3.2 NF Mutant line symbiosis assays - general

In total, two symbiosis assays with three separate time points per assay were completed for the NF18398 mutant line, which encodes for a putative NAC TF gene. These assays are represented in **Figures 3.2.2-3.2.3.** Statistically significant differences detected between mean colonization rates were observed in **Figure 3.2.2.**

Of the 216 plants used in the two symbiosis assays for NF18398, around 50% (108) were genotyped to ensure presence (Mutant type (MT)) or absence (WT) of the *Tnt1* insertion. A representative genotyping photo is shown in **Figure 3.2.1.**

In total, five symbiosis assays with two-three time points per assay were completed for the NF18424 mutant line, which encoded the *PALM1* gene. These assays are depicted in **Figures 3.2.4-3.2.8.** Statistically significant differences detected between mean colonization rates were observed in **Figures 3.2.4-3.2.8.**

Due to the five-leaflet per leaf phenotype expressed by *PALM1* mutants, genotyping was unnecessary, as the presence (MT) or absence (WT) of the *Tnt1* insertion could be ascertained by visual inspection of plants.

3.2.1. NF18398 symbiosis assay

The first symbiosis assay conducted to screen the NF18398 mutant line (**Figure 3.2.2**) demonstrated significant statistical decrease ($p < 0.05$) in mean root length colonization rates at 6 weeks post planting (wpp) between the mutant and the segregating WT (26.29% and 21.48%, respectively). Based on these results, a repetition of this experiment was conducted to determine if the trend was reproducible.

The second assay (**Figure 3.2.3**) did not show a statistically significant difference in mean root length colonization rates between the mutant and the segregating WT at 2 wpp (1.22 and 1.73), 3 wpp (4.00 and 4.04) or 6 wpp (19.68 and 20.71). Due to time restraints and the COVID19 pandemic, this experiment was not repeated for a third time.

3.2.1.2 NF18424 symbiosis assay

The first symbiosis assay conducted to screen the NF18424 mutant line (**Figure 3.2.4**) demonstrated significant statistical increase ($p < 0.05$) in mean root length colonization rates at 4 wpp between the mutant and the segregating WT (5.56% and 10.97%, respectively). Based on these results, a repetition of this experiment was conducted to determine if the trend was reproducible.

The second symbiosis assay (**Figure 3.2.5**) indicated a significant statistical increase ($p < 0.05$) in mean root length colonization rates at 4 wpp between the mutant and the segregating WT (10.01% and 4.07%, respectively), and at 5 wpp between the mutant and the segregating WT (32.69% and 14.20%, respectively). Based on these results, a third repetition of this experiment with earlier timepoints (due to the significance being found at earlier timepoints in the initial experiments) was conducted to confirm the reproducibility of these results.

The third symbiosis assay (**Figure 3.2.6**) indicated a significant increase ($p < 0.05$) in mean root length colonization rates at both 2.5 wpp and 4 wpp when comparing the mutant to the segregating WT and the R108 WT control (6.72%, 0.78% and 0.84% at 2.5 wpp, respectively), (23.79%, 12.17% and 11.63% at 4 wpp, respectively).

3.2.1.3 NF18424 leaf excision symbiosis assays

Leaflet excision for the excision experiment was conducted by hand, where one-two leaflets were randomly removed per leaf. The first leaf excision symbiosis assay conducted to screen the NF18424 mutant line (**Figure 3.2.7**) demonstrated significant statistical increase ($p < 0.05$) in mean root length colonization rates at 2 wpp between the 5-leaflet mutant and the segregating WT (7.57% and 3.52%, respectively). The five-leaflet mutant demonstrated significant statistical increase ($p < 0.05$) in mean root length colonization rates at 5 wpp when compared to the segregating WT and the R108 control (31.56%, 9.72%, and 10.54% respectively). The four-leaflet mutant demonstrated significant statistical increase ($p < 0.05$) in mean root length colonization rates at 5 wpp when compared to the segregating WT and the R108 control (30.53%, 9.72%, and 10.54% respectively). The five-leaflet mutant demonstrated significant statistical increase ($p < 0.05$) in mean root length colonization rates at 6 wpp when compared to the segregating WT and the R108 control (36.73%, 11.65%, and 12.59% respectively). The four-leaflet mutant demonstrated significant statistical increase ($p < 0.05$) in mean root length colonization rates at 6 wpp when compared to the segregating WT and the R108 control (35.68%, 11.65%, and 12.59% respectively). The three-leaflet mutant did not demonstrate significant statistical difference ($p > 0.05$) when compared to the segregating WT and the R108 control at any time point. Based on these results, a repetition of this experiment was conducted to determine if the trend was reproducible.

The second leaf excision symbiosis assay conducted to screen the NF18424 mutant line (**Figure 3.2.8**) demonstrated significant statistical increase ($p < 0.05$) in mean root length colonization rates at 5 wpp for the five-leaflet mutant compared to the segregating WT and the R108 control (29.23%, 11.11%, and 8.48% respectively). The four-leaflet mutant demonstrated significant statistical increase ($p < 0.05$) in mean root length colonization rates at 5 wpp when compared to the segregating WT and the R108 control (28.43%, 11.11%, and 8.48% respectively). The five-leaflet mutant demonstrated significant statistical increase ($p < 0.05$) in mean root length colonization rates at 6 wpp when compared to the segregating WT and the R108 control (34.44%, 12.36%, and 11.28% respectively). The four-leaflet mutant demonstrated significant statistical increase ($p < 0.05$) in mean root length colonization rates at 6 wpp when compared to the segregating WT and the R108 control (31.39%, 12.36%, and 11.28% respectively). The three-leaflet mutant did not demonstrate significant statistical difference ($p > 0.05$) when compared to the segregating WT and the R108 control at any time point.

3.3 Root phenotyping assays

One root phenotyping assay with one-time point at two weeks was conducted for NF18398 (represented in **Figures 3.3.1-3.3.9**) and NF18424 (**Figures 3.3.10-3.3.18**) *Tnt1* homozygous mutants.

3.3.1 NF18398 root phenotyping assay

Statistical analyses did not demonstrate significant variances when comparing the length of longest root, total root length, number of root tips, fresh root mass, fresh shoot mass, total fresh mass, total dry mass, dry shoot mass and dry root mass of the NF18398 mutant compared to the controls. The NF18398 mutant did not demonstrate any significant root phenotype when compared to the segregating WT and the R108 control plants.

3.3.2 NF18424 root phenotyping assay

At harvest, The NF18424 mutant demonstrated a significant increase ($p < 0.05$) in dry root mass when compared to the segregating WT and the R108 control plants (4.92 mg, 1.59 mg, and 1.72 mg, respectively) (**Figure 3.3.16**). In addition, the NF18424 mutant demonstrated a significant decrease ($p < 0.05$) in dry shoot mass when compared to the segregating WT and the R108 control plants (0.95 mg, 2.785 mg, and 3.44 mg, respectively) (**Figure 3.3.17**).

3.4 Leaf Surface Area Analyses

A comparison of mean leaf surface area between the NF18424 mutant with five leaflets per leaf, NF18424 mutant with four leaflets per leaf (one leaflet removed), NF18424 mutant with three leaflets per leaf (two leaflets removed), the NF18424 segregating WT and the R108 WT, all inoculated with *Rhizophagus irregularis* at one-time point (5 wpp) did not indicate any statistical significance (**Figure 3.4.1**). Statistically, the five-leaflet mutant was similar in leaf surface area to the segregating WT and the R108 WT control. The four-leaflet and three-leaflet mutant plants showed a decrease in surface area when compared to the five-leaflet mutant, the segregating WT and the R108 control plants (1.24 cm^2, 1.20 cm^2, 1.73 cm^2, 1.67 cm^2, and 1.56

cm², respectively) but this difference was not statistically significant. This experiment was repeated a second time with additional time points to assess whether the trend was reproducible.

In the second leaf surface area experiment, the leaf surface area was measured at three-time points, including two weeks, five weeks, and six weeks post-planting (**Figure 3.4.2**). At two weeks post-planting, the three-leaflet mutant demonstrated significantly ($p < 0.05$) decreased surface area when compared to both the segregating WT and the R108 control (0.93 cm², 1.36 cm², and 1.89 cm², respectively). The four leaflet and five leaflet mutants did not show a significant difference in surface area when compared to the control plants. At five weeks post-planting, the three-leaflet mutant demonstrated significantly ($p < 0.05$) decreased surface area when compared to both the segregating WT and the R108 control (1.29 cm², 2.21 cm², and 2.36 cm², respectively). The four leaflet and five leaflet mutants did not show significant difference in surface areas when compared to the control plants. At six weeks post-planting, the three-leaflet mutant demonstrated significantly ($p < 0.05$) decreased surface area when compared to both the segregating WT and the R108 control (1.69 cm², 2.65 cm², and 2.30 cm², respectively). The four leaflet and five leaflet mutants did not show significant difference in overall leaf surface area when compared to the control plants.

In addition, a comparison of total fresh mass, fresh shoot mass, fresh root mass, dry shoot mass (**Figure 3.4.3-3.4.6**) between the NF18424 mutant with five leaflets per leaf, NF18424 mutant with four leaflets per leaf (one leaflet removed), NF18424 mutant with three leaflets per leaf (two leaflets removed), the NF18424 segregating WT and the R108 WT inoculated with *Rhizophagus irregularis* at one-time point (5 wpp) did not indicate any statistically significant differences.

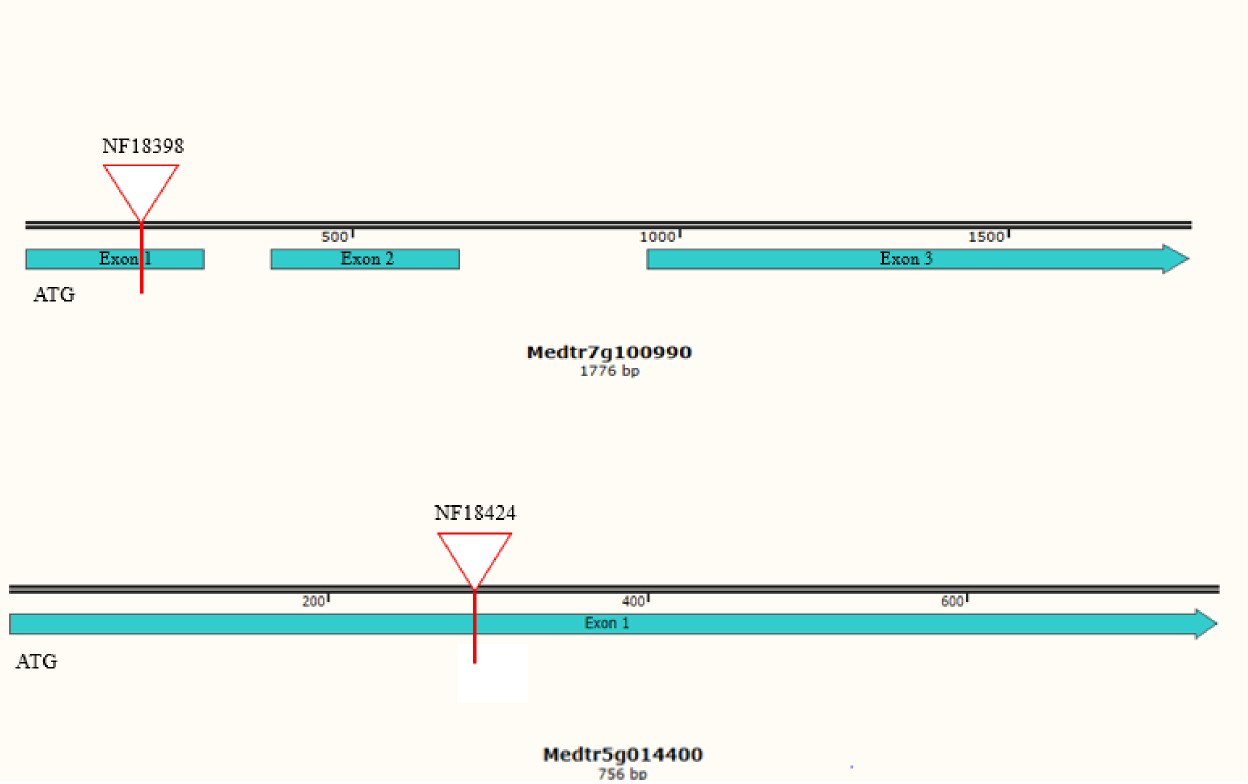

Figure 3.1. Insertion sites of two *Tnt1* mutants into two genes of interest. The Blue boxes indicate exons, ATG indicates the start codon, red line indicates the location of the Tnt1 insertion.

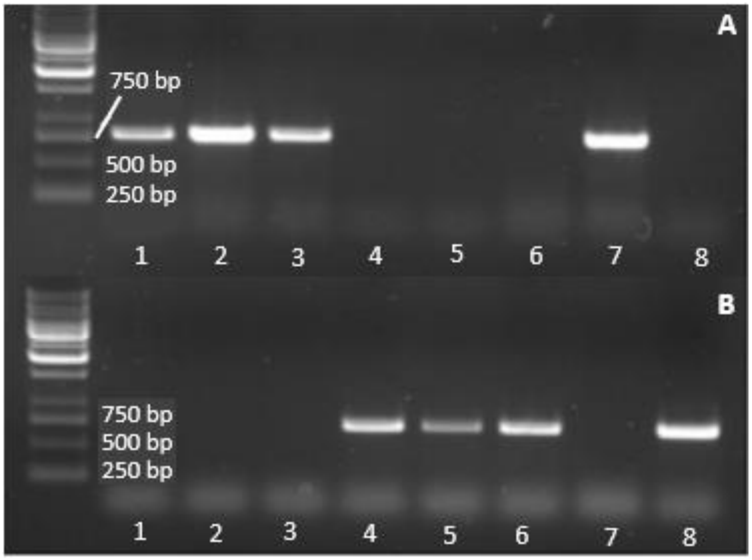

Figure 3.2.1. Representative image of genotyping of transgenic line NF18398 (*Medtr7g100990*) via PCR. Panel A primers: NF18398_R + Tnt1 R (expected size: 749 bp). Panel B primers: NF18398_F + NF18398_R combination (expected size: 788 bp). Lanes 1-3 depict PCR completed on Tnt1 homozygous plants, as expected. Lanes 4-6 depict PCR completed with DNA from segregating WT plants at the gene of interest, as expected. Lane 7 is a NF16380 Tnt1 homozygous positive control. Lane 8 is a R108 WT control.

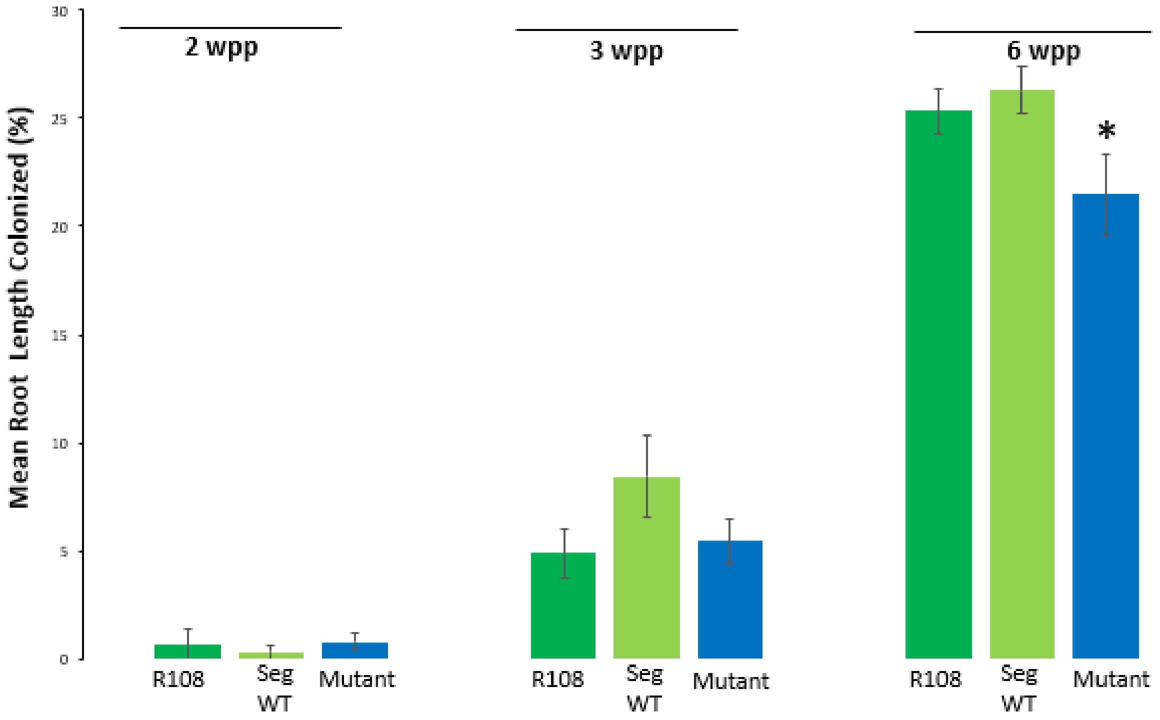

Figure 3.2.2 Results from NF18398 (NAC TF) Assay #1. Comparison of mean root length colonized between the NF18398 mutant, and the two Wild Type controls: the NF18398 segregating Wild Type and the R108 Wild Type, all inoculated with *Rhizophagus irregularis* at three time points (2 weeks, 3 weeks, and 6 weeks post planting (wpp)). Error bars indicate standard error, n = 18. Asterisks indicates p-value < 0.05 in a one-way ANOVA comparing mutants and control plants. T2:T3 p value = 0.02943

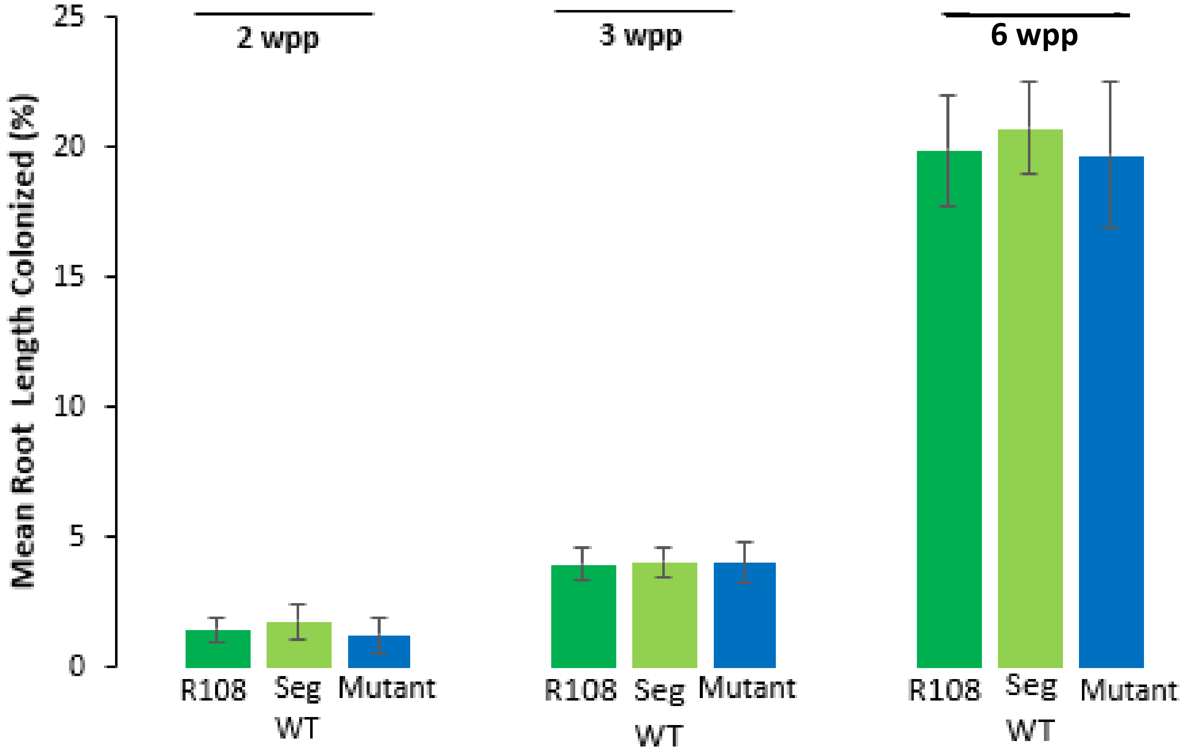

Figure 3.2.3 Results from NF18398 (NAC TF) Assay #2. Comparison of mean root length colonized between the NF18398 mutant, the NF18398 segregating Wild Type and the R108 Wild Type, all inoculated with *Rhizophagus irregularis* at three time points (2 weeks, 3 weeks, and 6 weeks post planting (wpp)). Error bars indicate standard error, n = 18.

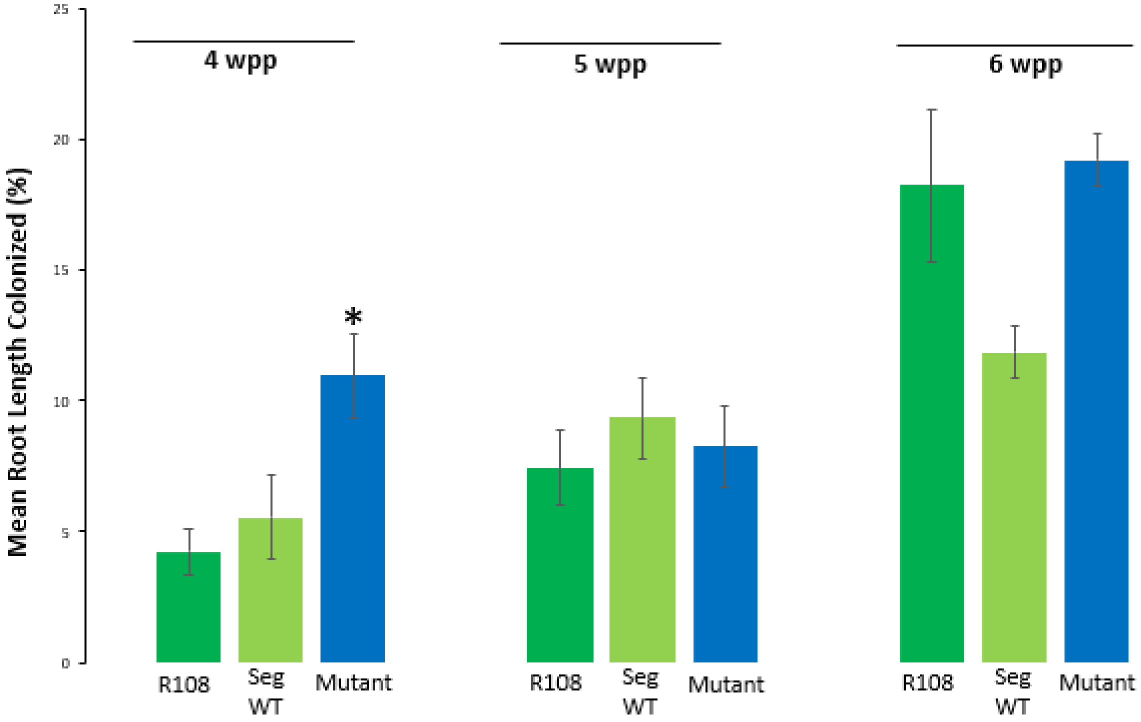

Figure 3.2.4 Results from NF18424 (*PALM1*) Assay #1. Comparison of mean root length colonized between the NF18424 mutant, the NF18424 segregating WT and the R108 WT, all inoculated with *Rhizophagus irregularis* at three time points (4 weeks, 5 weeks, and 6 weeks post planting (wpp)). Error bars indicate standard error, n = 18. Asterisks indicates p-value < 0.05 in a one-way ANOVA comparing mutants and control plants. T1:T3 p value = 0.03291

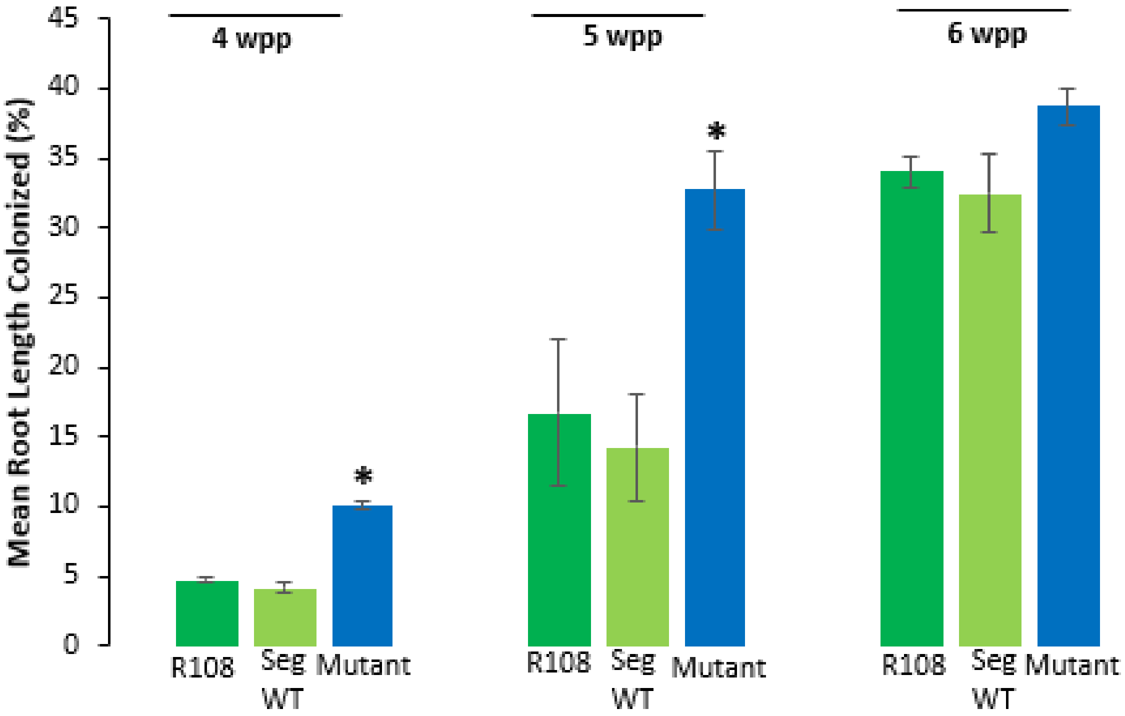

Figure 3.2.5 Results from NF18424 (*PALM1*) Assay #2. Comparison of mean root length colonized between the NF18424 mutant, the NF18424 segregating WT and the R108 WT, all inoculated with *Rhizophagus irregularis* at three time points (4 weeks, 5 weeks, and 6 weeks post planting (wpp)). Data shown is averaged and error bars indicate standard error, n = 18. Asterisks indicates p-value < 0.05 in a one-way ANOVA comparing mutants and control plants. 4 wpp: T1:T3 p value = 0.0000, T2:T3 p value = 0.0000. 5 wpp: T1:T3 p value = 0.02736, T2:T3 p value = 0.01011.

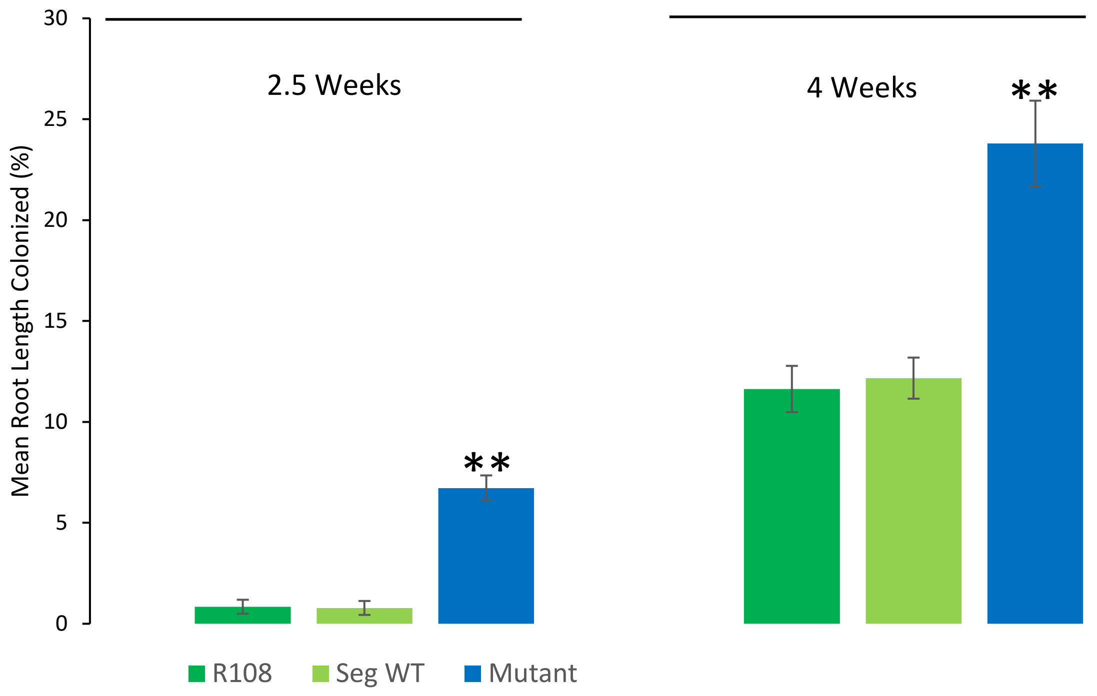

Figure 3.2.6. Results from NF18424 (*PALM1*) Assay #3. Comparison of mean root length colonized between the NF18424 mutant, the NF18424 segregating WT and the R108 WT, all inoculated with *Rhizophagus irregularis* at two time points: 2.5 weeks and 4 weeks post planting (wpp). Data shown is averaged and error bars indicate standard error, n = 18. Asterisks indicates p-value < 0.05 in a one-way ANOVA comparing mutants and control plants. 2.5 wpp: T1:T3 p-value: 0.00000. 4 wpp: T2:T3 p-value: 0.00000.

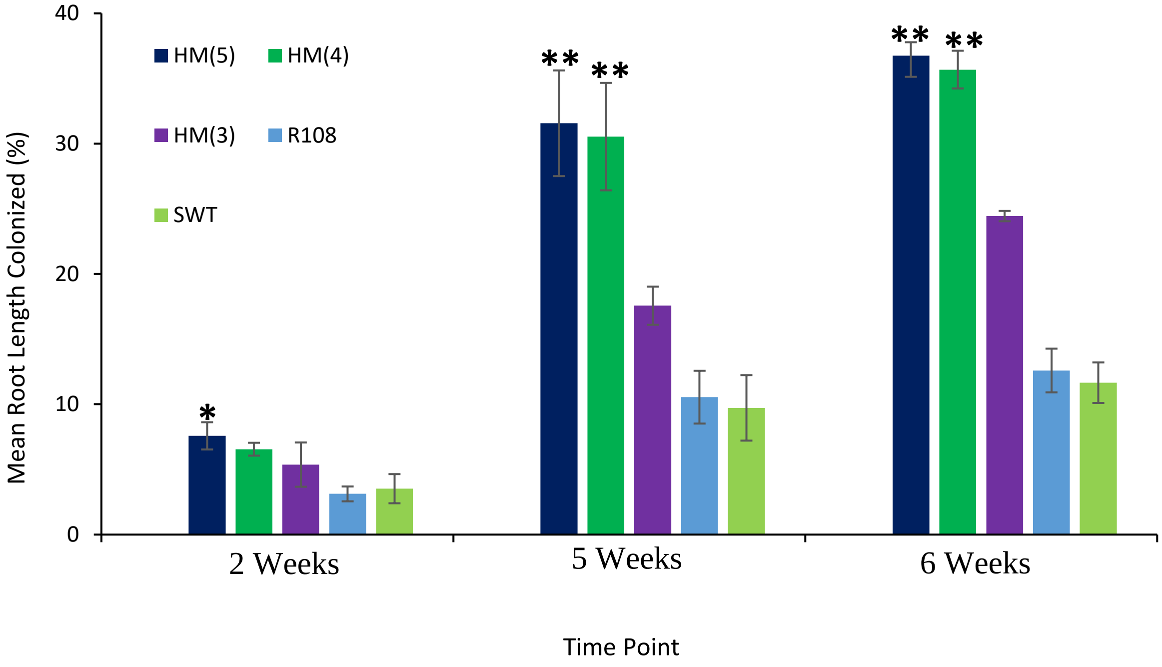

Figure 3.2.7. Results from NF18424 (*PALM1*) Leaf Excision Assay #1. Comparison of mean root length colonized between the NF18424 mutant with leaves of five leaflets, the NF18424 mutant with leaves of four leaflets, and the NF18424 mutant with leaves of three leaflets, the NF18424 segregating WT and the R108 WT, all inoculated with *Rhizophagus irregularis* at three time points: 2 wpp, 5 wpp, and 6 wpp. Error bars indicate standard error, n = 18. Asterisks indicates p-value < 0.05 in a one-way ANOVA comparing mutants and control plants. 2 wpp: T1:T4 p-value: .04249. 5 wpp: T1:T4 p-value: 0.00018, T1:T5 p-value: 0.00010, T2:T4 p-value: 0.00038 T2:T5 p-value: 0.00021. 6 wpp: T1:T4 p-value: 0.00000, T1:T5 p-value: 0.00000, T2:T4 p-value: 0.00000 T2:T5 p-value: 0.00000.

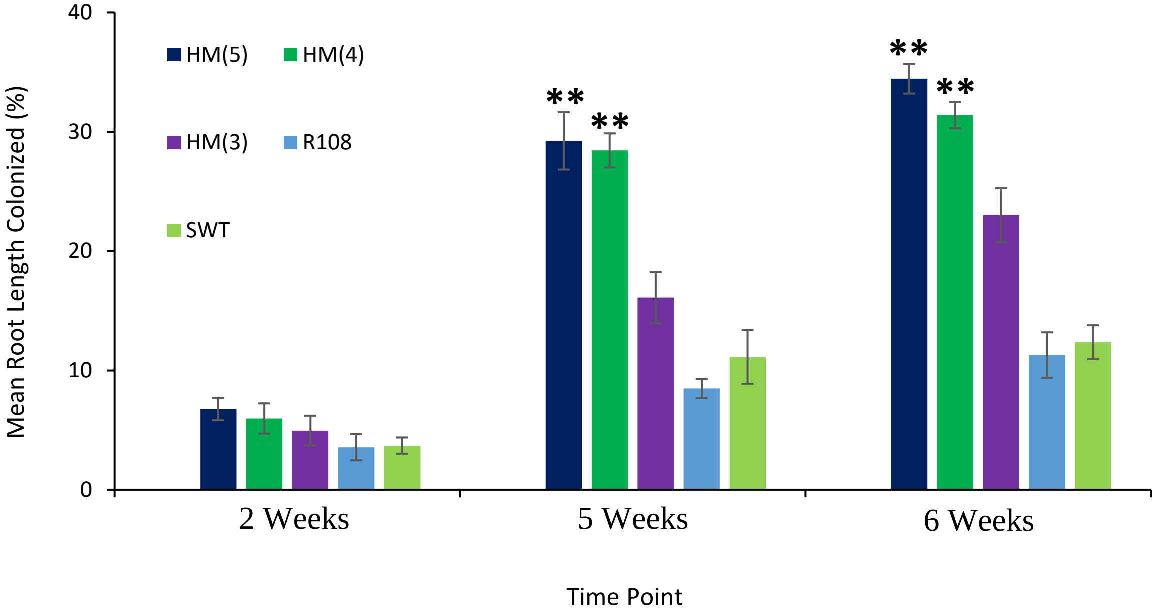

Figure 3.2.8. Results from NF18424 (*PALM1*) Leaf Excision Assay #2. Comparison of mean root length colonized between the NF18424 mutant with leaves of five leaflets, the NF18424 mutant with leaves of four leaflets, and the NF18424 mutant with leaves of three leaflets, the NF18424 segregating WT and the R108 WT, all inoculated *with Rhizophagus irregularis* at three time points: 2 wpp, 5 wpp, and 6 wpp. Error bars indicate standard error, n = 18. Asterisks indicates p-value < 0.05 in a one-way ANOVA comparing mutants and control plants. 5 wpp: T1:T4 p-value: 0.00000, T1:T5 p-value: 0.00000, T2:T4 p-value: 0.00000 T2:T5 p-value: 0.00000. 6 wpp: T1:T4 p-value: 0.00000, T1:T5 p-value: 0.00000, T2:T4 p-value: 0.00000 T2:T5 p-value: 0.00000.

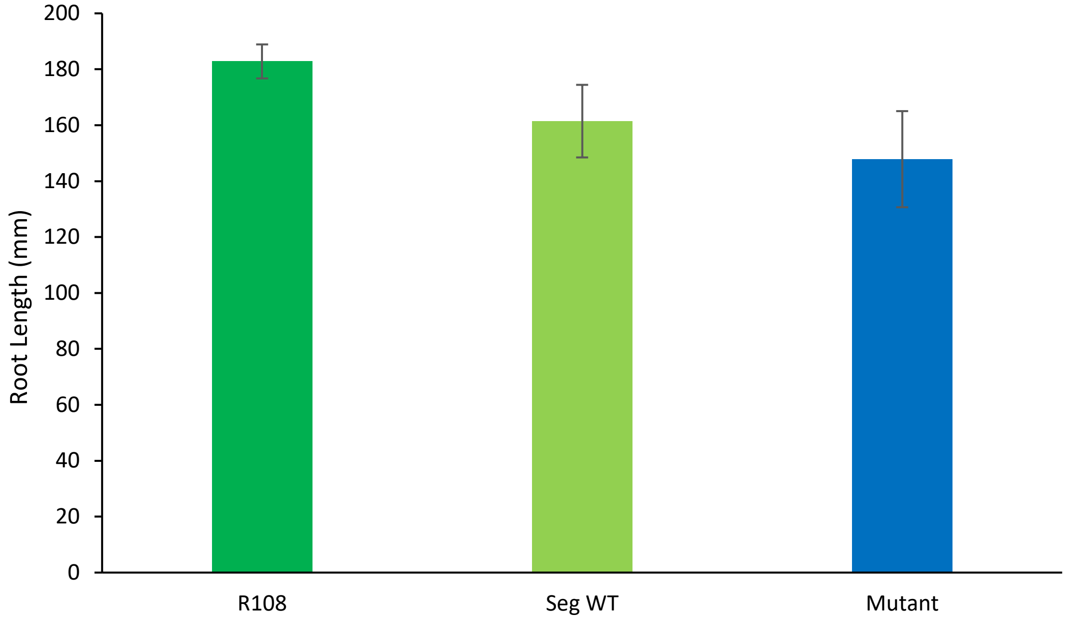

Figure 3.3.1 Results from NF18398 (NAC TF) Root Phenotyping Assay: Longest Root. Comparison of mean longest root between the NF18398 mutant, the NF18398 segregating WT and the R108 WT at one time point (2 wpp). Data shown is averaged and error bars indicate standard error, n = 20.

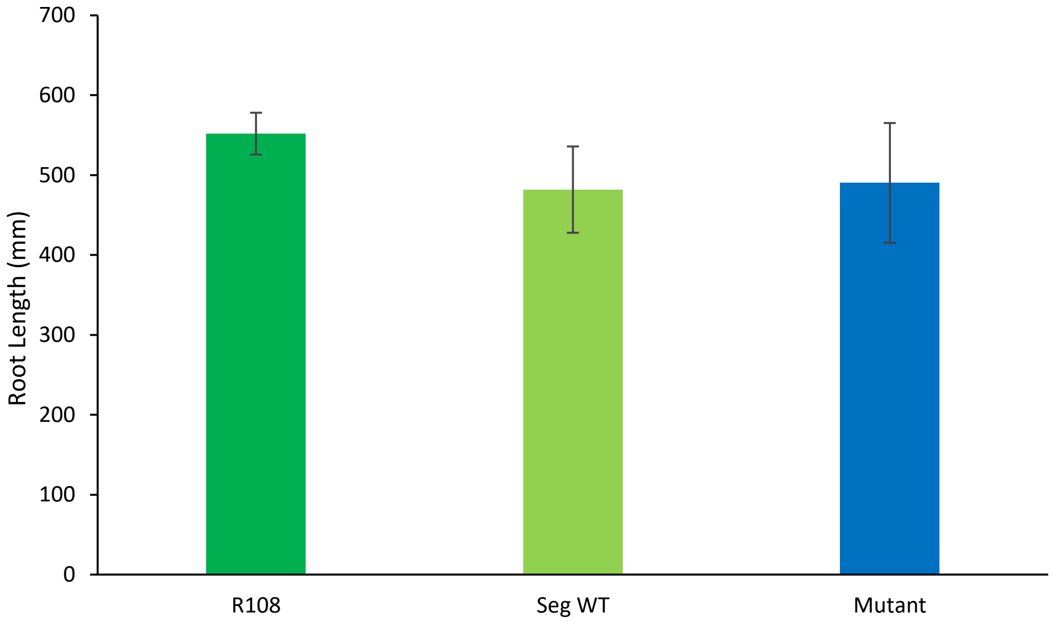

Figure 3.3.2. Results from NF18398 (NAC TF) Root Phenotyping Assay: Total Root Length. Comparison of total root length between the NF18398 mutant, the NF18398 segregating WT and the R108 WT at one time point (2 wpp). Data shown is averaged and error bars indicate standard error, n = 20.

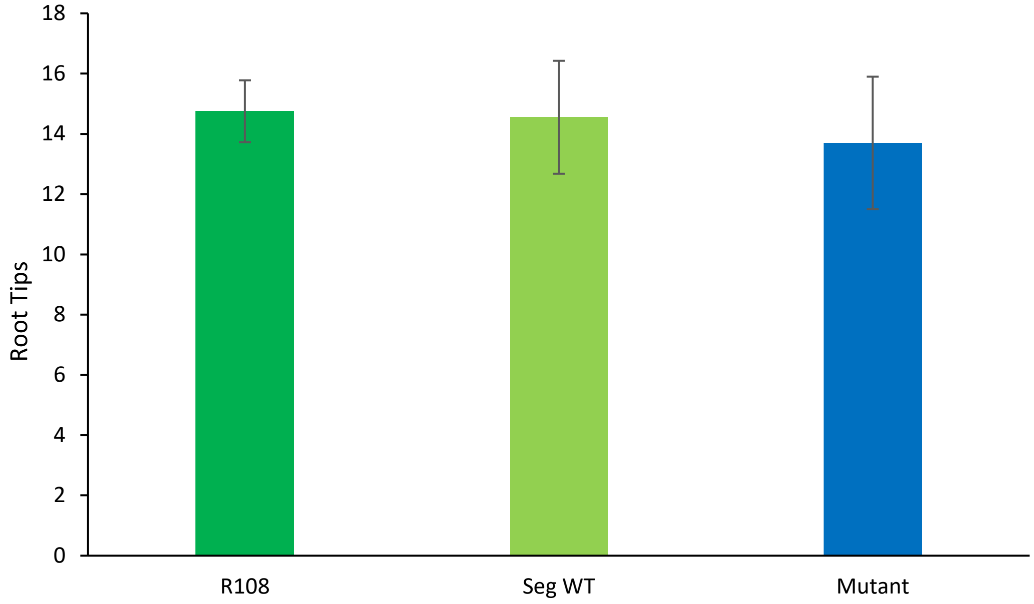

Figure 3.3.3 Results from NF18398 (NAC TF) Root Phenotyping Assay: Number of Total Root Tips. Comparison of total root tips between the NF18398 mutant, the NF18398 segregating WT and the R108 WT at one time point (2 wpp). Data shown is averaged and error bars indicate standard error, n = 20.

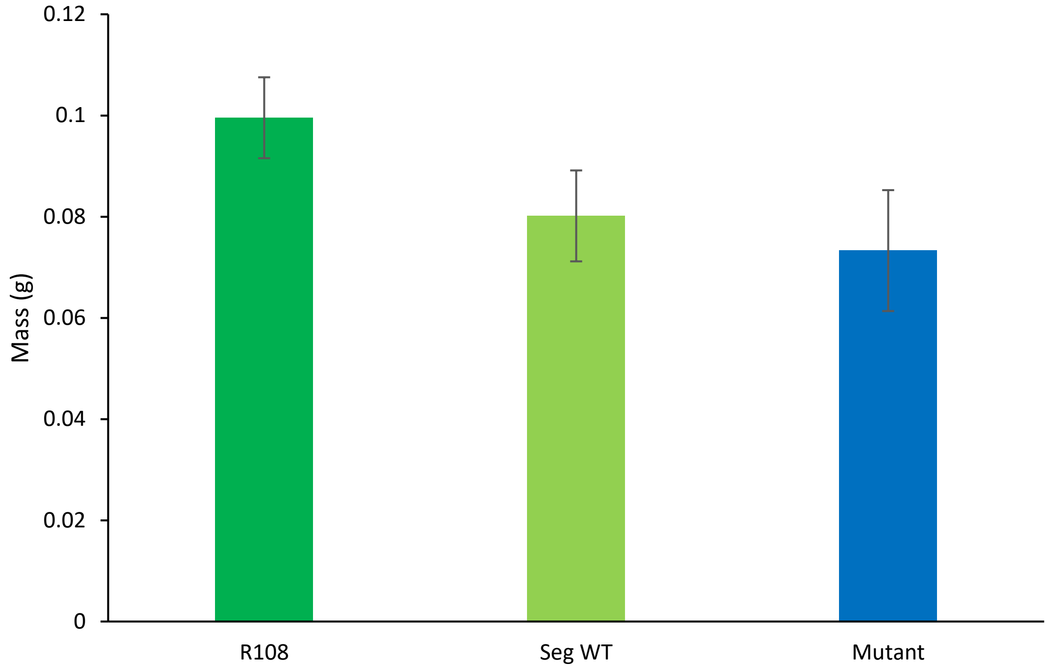

Figure 3.3.4 Results from NF18398 (NAC TF) Root Phenotyping Assay: Fresh Root Mass. Comparison of fresh root mass between the NF18398 mutant, the NF18398 segregating WT and the R108 WT at one time point (2 wpp). Data shown is averaged and error bars indicate standard error, n = 20.

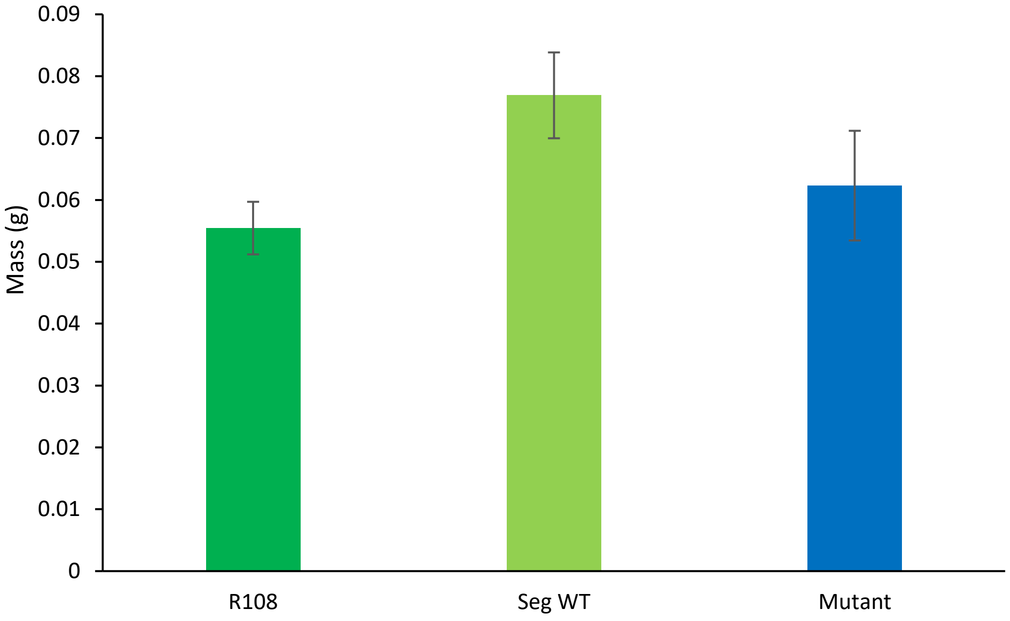

Figure 3.3.5 Results from NF18398 (NAC TF) Root Phenotyping Assay: Fresh Shoot Mass. Comparison of fresh shoot mass between the NF18398 mutant, the NF18398 segregating WT and the R108 WT at one time point (2 wpp). Data shown is averaged and error bars indicate standard error, n = 20.

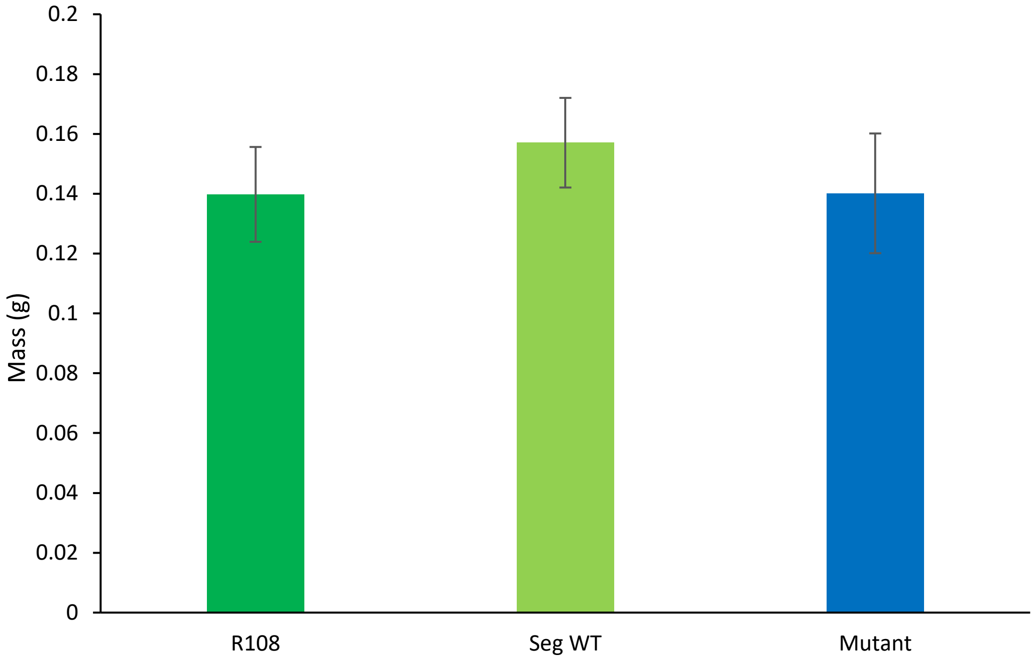

Figure 3.3.6 Results from NF18398 (NAC TF) Root Phenotyping Assay: Total Fresh Mass Comparison of total fresh mass between the NF18398 mutant, the NF18398 segregating WT and the R108 WT at one time point (2 wpp). Data shown is averaged and error bars indicate standard error, n = 20.

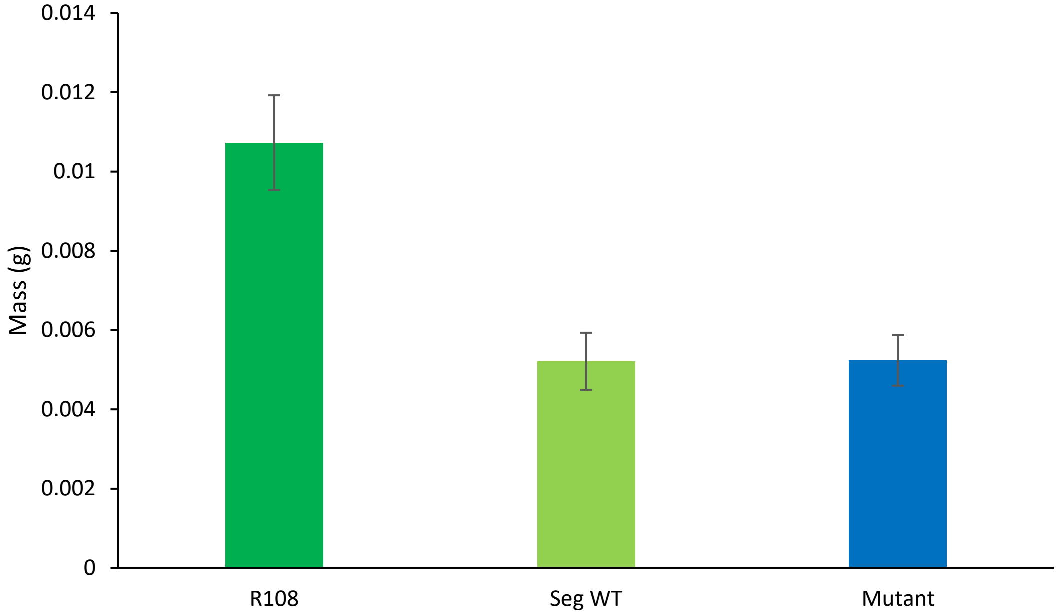

Figure 3.3.7 Results from NF18398 (NAC TF) Root Phenotyping Assay: Dry Root Mass Comparison of dry root mass between the NF18398 mutant, the NF18398 segregating WT and the R108 WT at one time point (2 wpp). Data shown is averaged and error bars indicate standard error, n = 20.

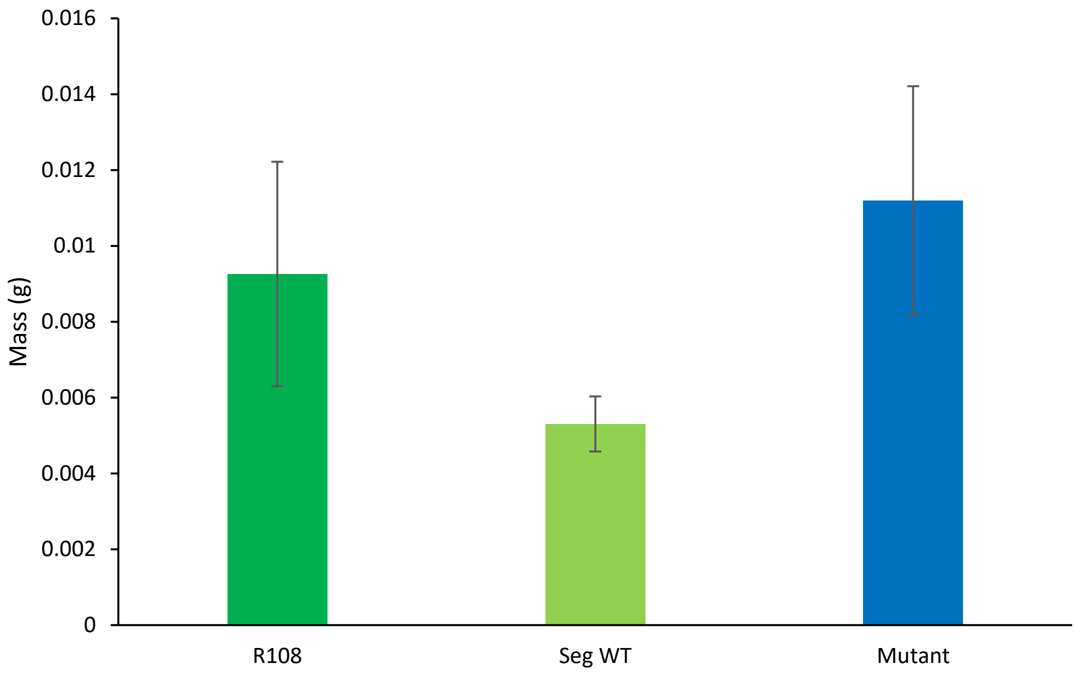

Figure 3.3.8 Results from NF18398 (NAC TF) Root Phenotyping Assay: Dry Shoot Mass Comparison of dry shoot mass between the NF18398 mutant, the NF18398 segregating WT and the R108 WT at one time point (2 wpp). Data shown is averaged and error bars indicate standard error, n = 20.

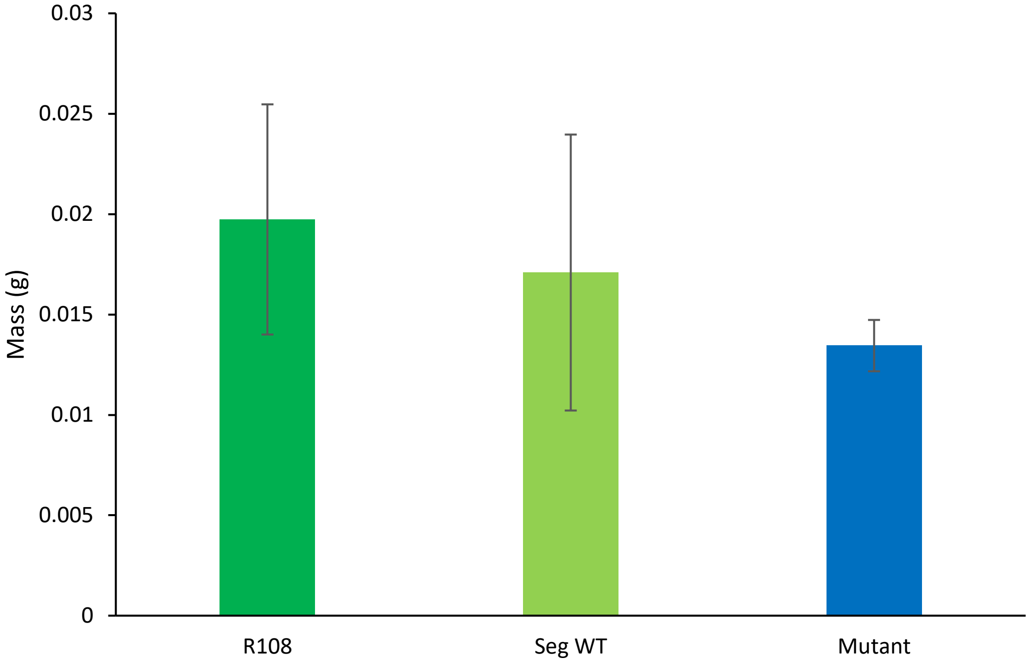

Figure 3.3.9 Results from NF18398 (NAC TF) Root Phenotyping Assay: Total Dry Mass. Comparison of total dry mass between the NF18398 mutant, the NF18398 segregating WT and the R108 WT at one time point (2 wpp). Data shown is averaged and error bars indicate standard error, n = 20.

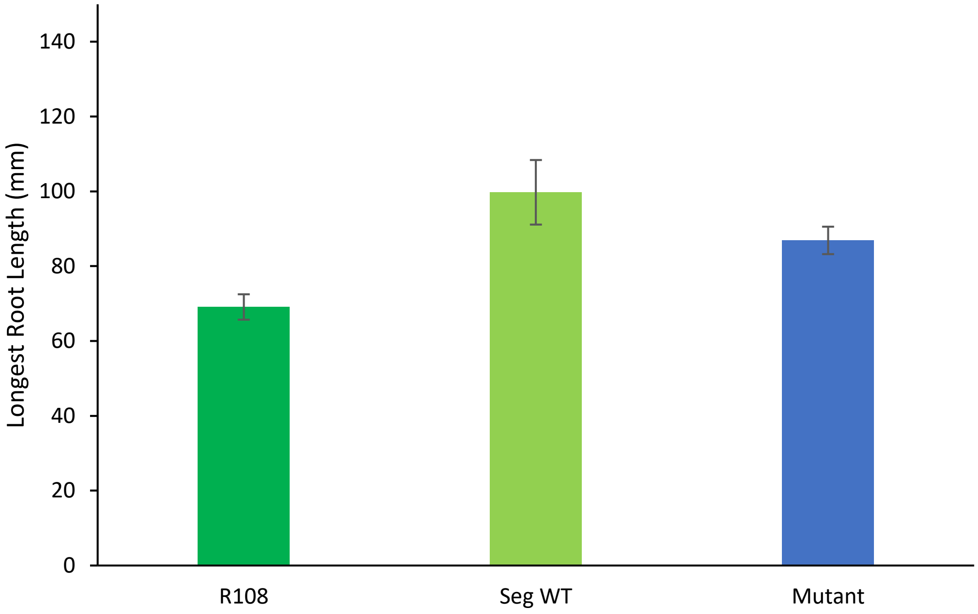

Figure 3.3.10 Results from NF18424 (*PALM1*) Root Phenotyping Assay: Longest Root Length. Comparison of mean longest root length between the NF18424 mutant, the NF18424 segregating WT and the R108 WT at one time point (2 wpp). Data shown is averaged and error bars indicate standard error, n = 20.

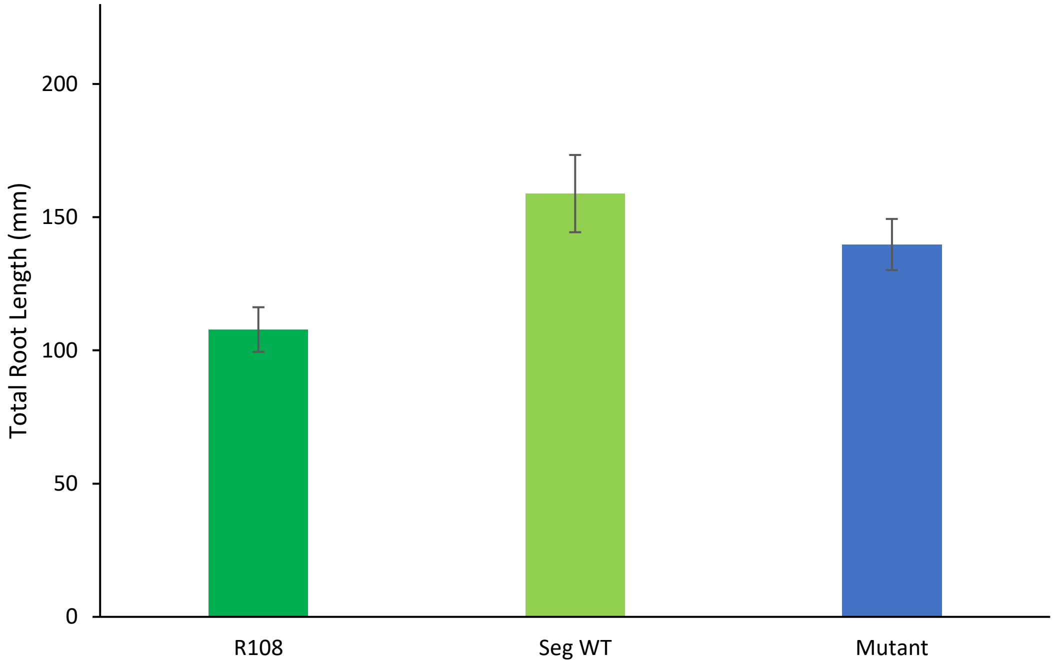

Figure 3.3.11 Results from NF18424 (*PALM1*) Root Phenotyping Assay: Total Root Length. Comparison of mean total root length between the NF18424 mutant, the NF18424 segregating WT and the R108 WT at one time point (2 wpp). Data shown is averaged and error bars indicate standard error, n = 20.

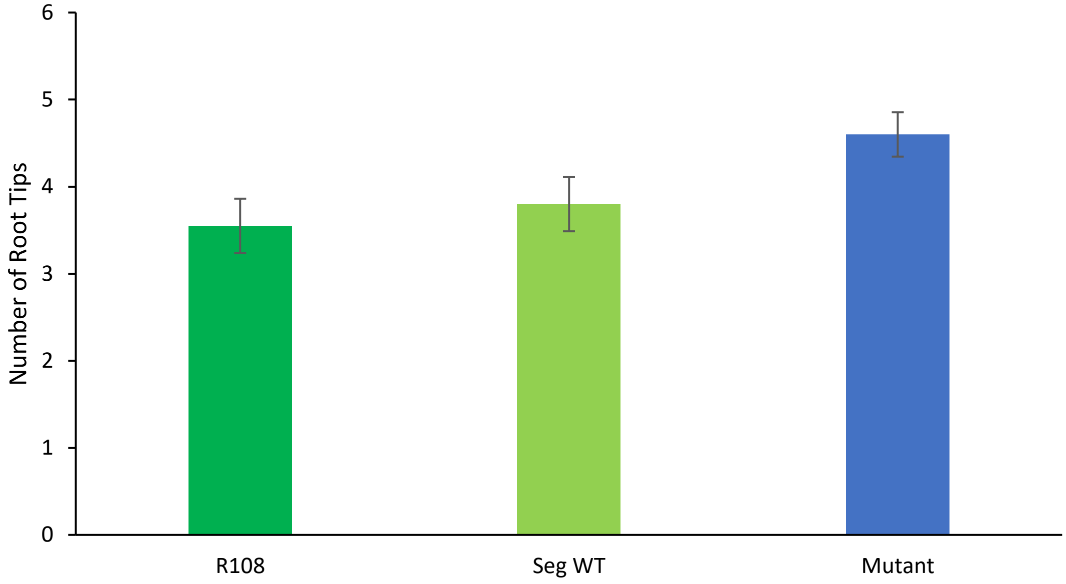

Figure 3.3.12 Results from NF18424 (*PALM1*) Root Phenotyping Assay: Total Root Tips. Comparison of mean total root tips between the NF18424 mutant, the NF18424 segregating WT and the R108 WT at one time point (2 wpp). Data shown is averaged and error bars indicate standard error, n = 20.

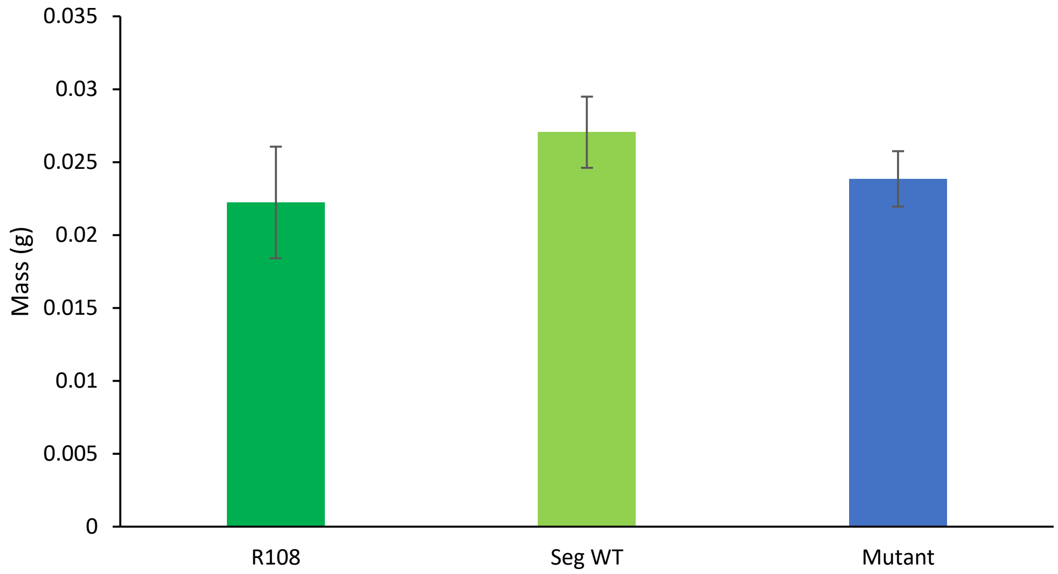

Figure 3.3.13 Results from NF18424 (*PALM1*) Root Phenotyping Assay: Total Fresh Root Mass. Comparison of mean total fresh root mass between the NF18424 mutant, the NF18424 segregating WT and the R108 WT at one time point (2 wpp). Data shown is averaged and error bars indicate standard error, n = 20.

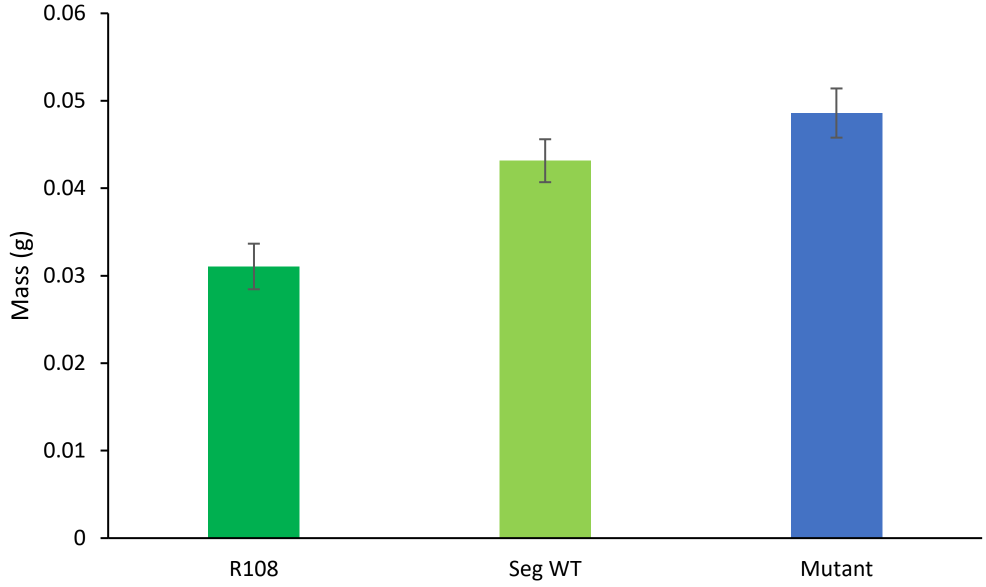

Figure 3.3.14 Results from NF18424 (*PALM1*) Root Phenotyping Assay: Total Fresh Shoot Mass. Comparison of mean total fresh shoot mass between the NF18424 mutant, the NF18424 segregating WT and the R108 WT at one time point (2 wpp). Data shown is averaged and error bars indicate standard error, n = 20.

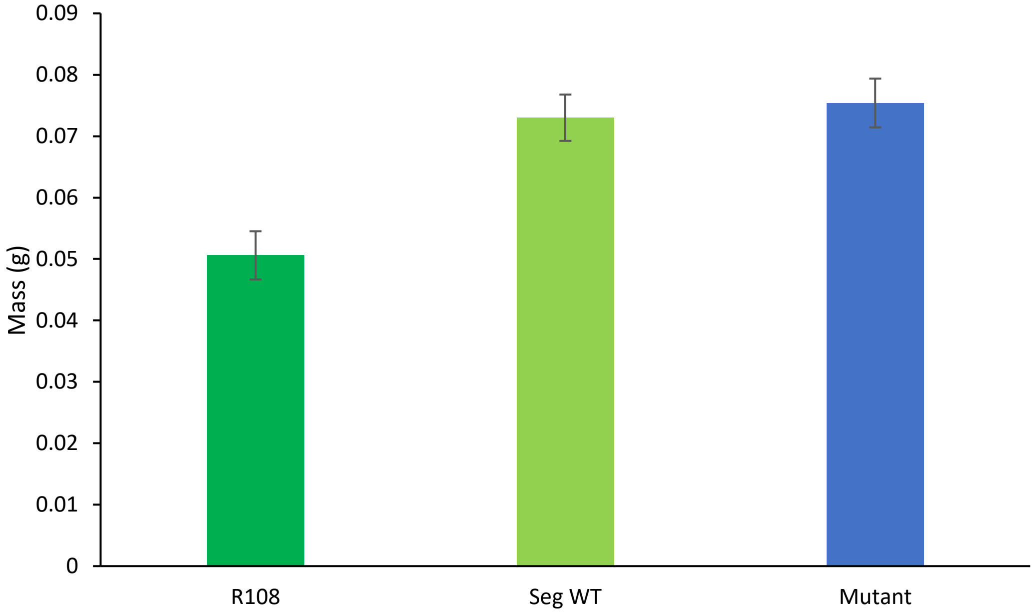

Figure 3.3.15 Results from NF18424 (*PALM1*) Root Phenotyping Assay: Total Fresh Mass. Comparison of mean total fresh mass between the NF18424 mutant, the NF18424 segregating WT and the R108 WT at one time point (2 wpp). Data shown is averaged and error bars indicate standard error, n = 20.

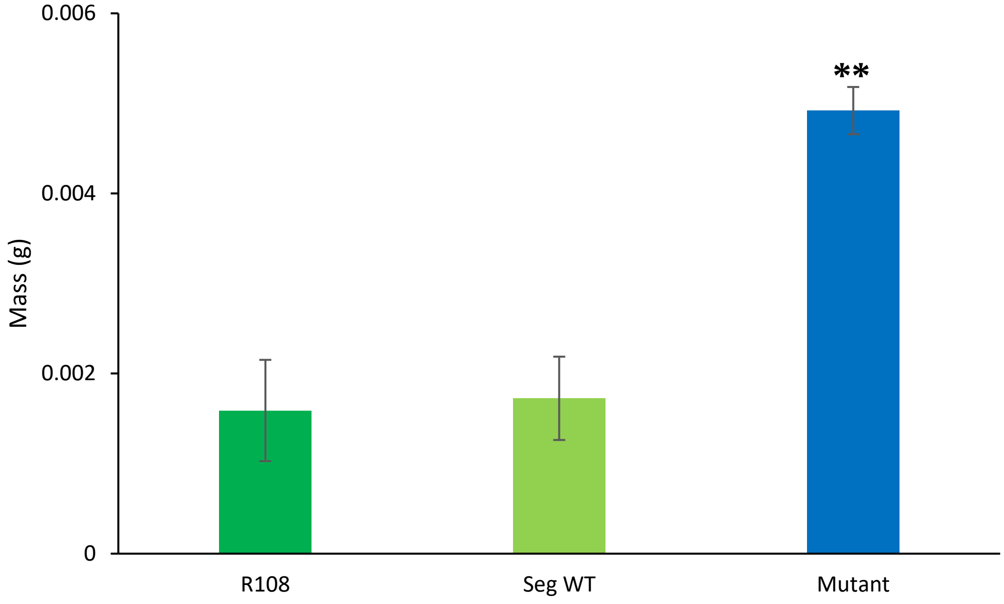

Figure 3.3.16 Results from NF18424 (*PALM1*) Root Phenotyping Assay: Dry Root Mass. Comparison of mean dry root mass between the NF18424 mutant, the NF18424 segregating WT and the R108 WT at one time point (2 wpp). Error bars indicate standard error, n = 20. Asterisks indicates p-value < 0.05 in a one-way ANOVA comparing mutants and control plants. T1:T2 p value = 0.98628, T1:T3 p value = 0.0001 and T2:T3 p value = 0.0001.

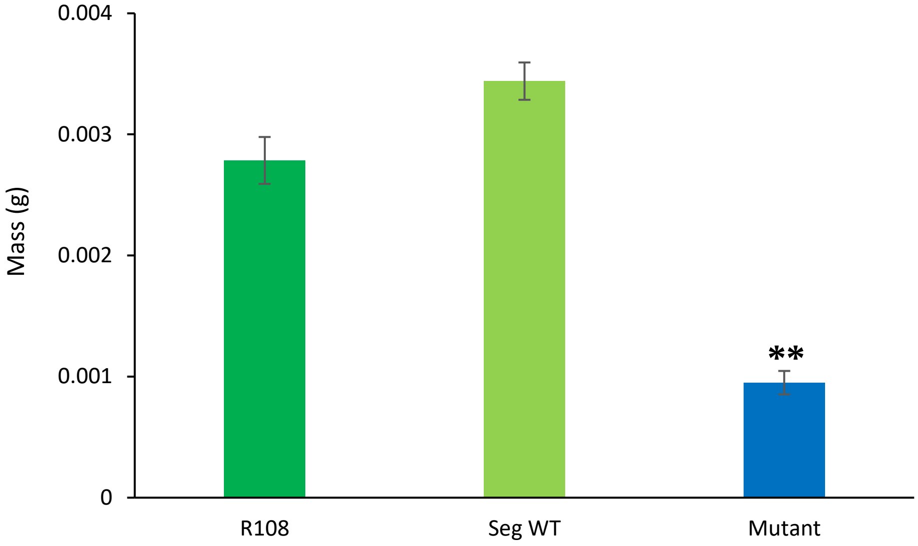

Figure 3.3.17 Results from NF18424 (*PALM1*) Root Phenotyping Assay: Dry Shoot Mass. Comparison of mean dry shoot mass between the NF18424 mutant, the NF18424 segregating WT and the R108 WT at one time point (2 wpp). Error bars indicate standard error, n = 20. Asterisks indicates p-value < 0.05 in a one-way ANOVA comparing mutants and control plants. T1:T2 p value = 0.02056, T1:T3 p value = 0.0000 and T2:T3 p value = 0.0000.

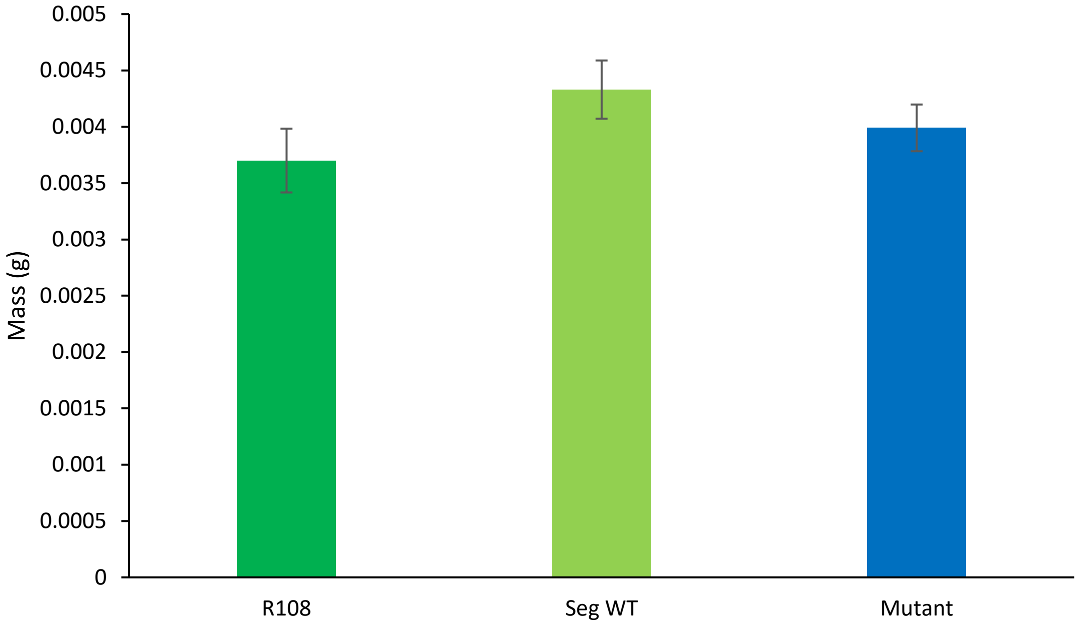

Figure 3.3.18 Results from NF18424 (*PALM1*) Root Phenotyping Assay: Total Dry Mass. Comparison of mean total dry mass between the NF18424 mutant, the NF18424 segregating WT and the R108 WT at one time point (2 wpp). Data shown is averaged and error bars indicate standard error, n = 20.

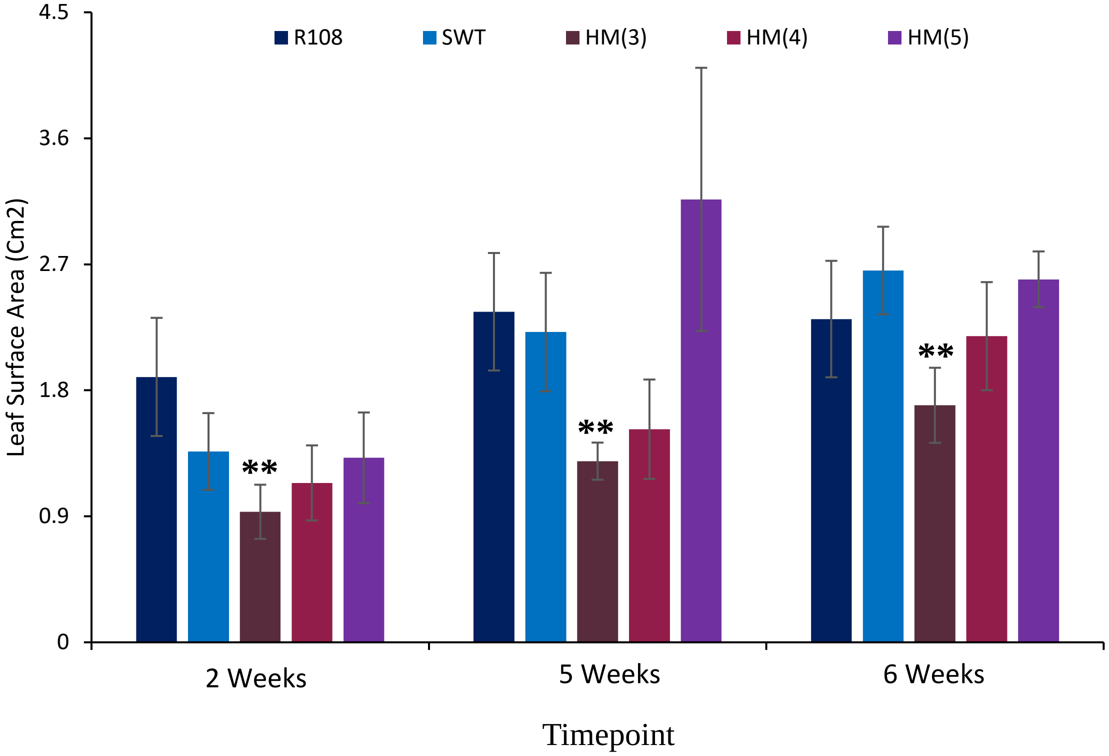

Figure 3.4.1 Results from NF18424 (*PALM1*) Leaf Surface Area Experiment (Second Assay). Comparison of mean leaf surface area between the NF18424 mutant with five leaflets, NF18424 mutant with four leaflets per leaf (one leaflet removed), NF18424 mutant with three leaflets per leaf (two leaflets removed), the NF18424 segregating WT and the R108 WT, all inoculated with *Rhizophagus irregularis* at three-time point (2 wpp, 5 wpp, and 6 wpp). Error bars indicate standard error, n = 18. Asterisks indicates p-value < 0.05 in a one-way ANOVA comparing mutants and control plants. 2 wpp: T1:T3 p = 0.00000 & T2:T3 p = 0.00056. 5 wpp: T1:T3 p = 0.00000 & T2:T3 p = 0.00000. 6 wpp: T1:T3 p = 0.00000 & T2:T3 p = 0.00000.

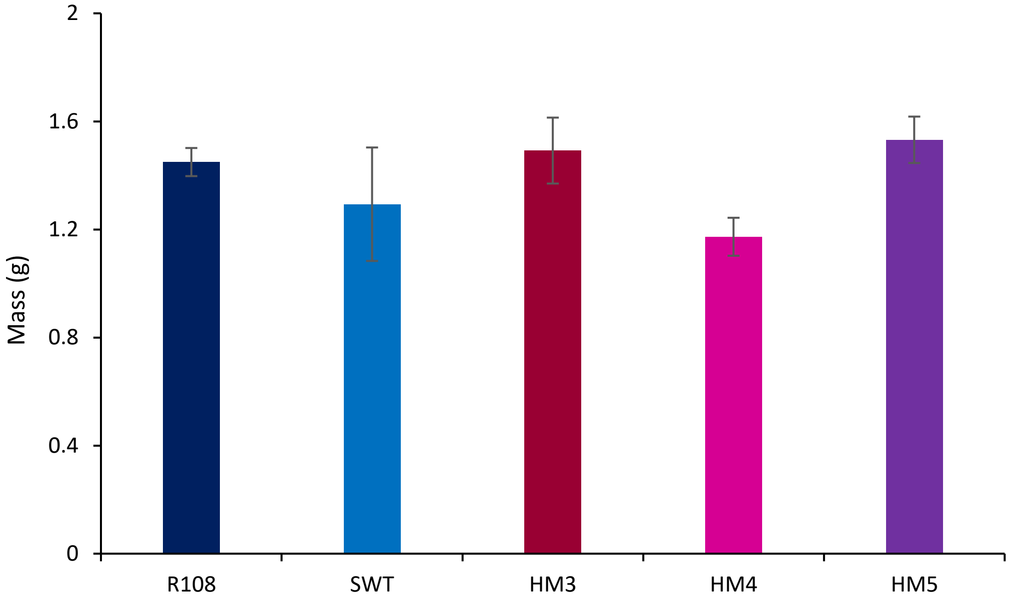

Figure 3.4.2 Results from NF18424 (*PALM1*): Total Fresh Mass. Comparison of fresh root mass between the NF18424 mutant with five leaflets, NF18424 mutant with four leaflets per leaf (one leaflet removed), NF18424 mutant with three leaflets per leaf (two leaflets removed), the NF18424 segregating WT and the R108 WT, all inoculated with *Rhizophagus irregularis* at one time point (5 weeks post planting). Error bars indicate standard error, n = 18.

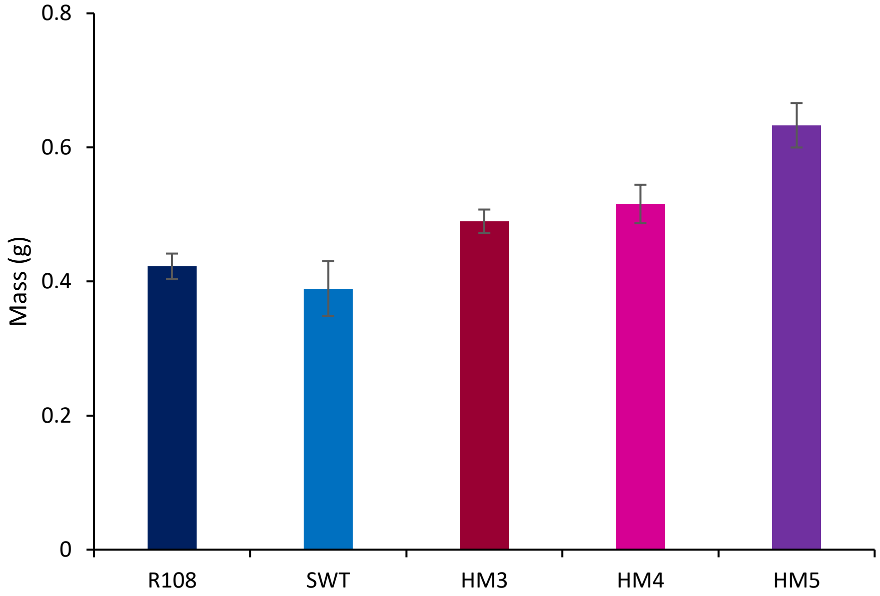

Figure 3.4.3 Results from NF18424 (*PALM1*): Fresh Shoot Mass. Comparison of fresh root mass between the NF18424 mutant with five leaflets, NF18424 mutant with four leaflets per leaf (one leaflet removed), NF18424 mutant with three leaflets per leaf (two leaflets removed), the NF18424 segregating WT and the R108 WT, all inoculated with *Rhizophagus irregularis* at one time point (5 weeks post planting). Error bars indicate standard error, n = 18.

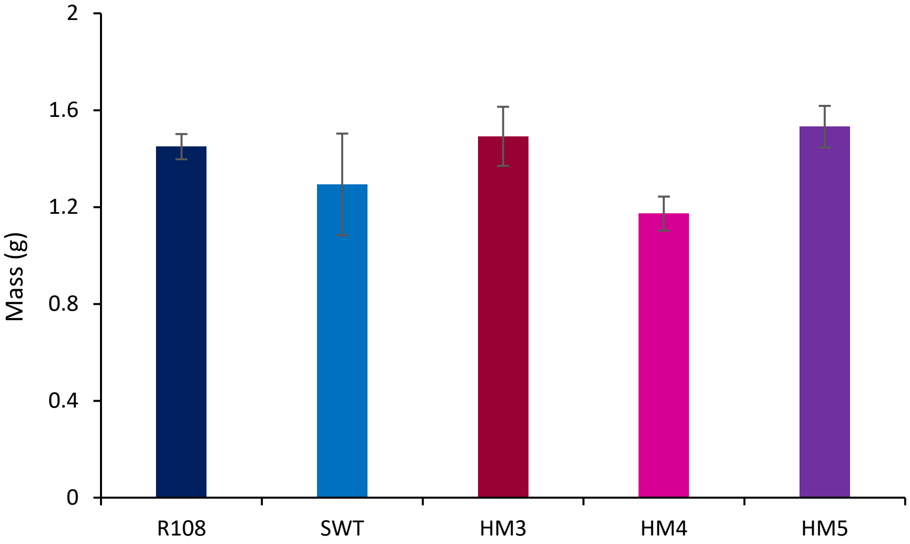

Figure 3.4.4 Results from NF18424 (*PALM1*): Fresh Root Mass. Comparison of fresh root mass between the NF18424 mutant with five leaflets, NF18424 mutant with four leaflets per leaf (one leaflet removed), NF18424 mutant with three leaflets per leaf (two leaflets removed), the NF18424 segregating WT and the R108 WT, all inoculated with *Rhizophagus irregularis* at one time point (5 weeks post planting). Error bars indicate standard error, n = 18.

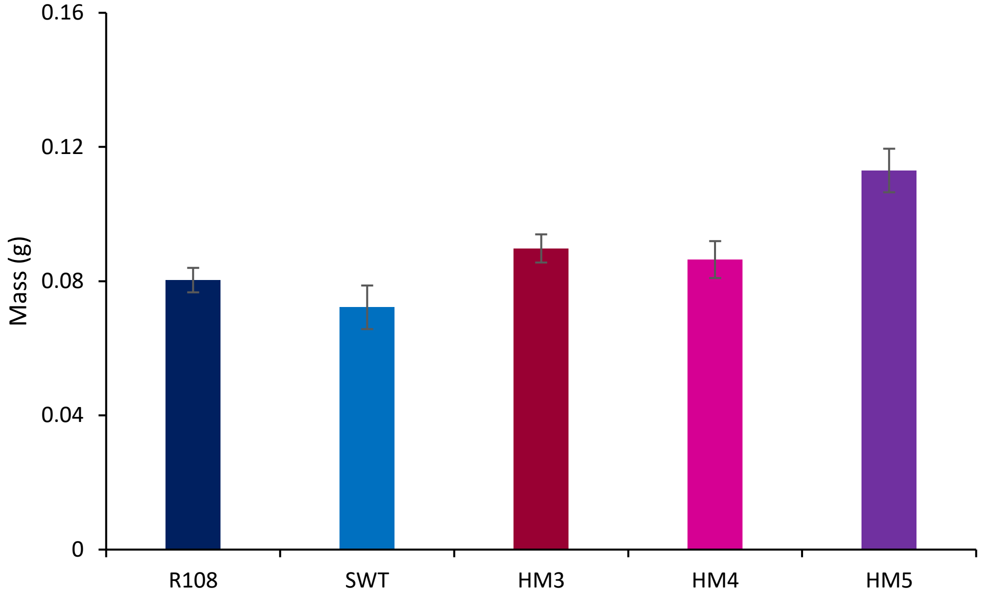

Figure 3.4.5 Results from NF18424 (*PALM1*): Dry Shoot Mass. Comparison of fresh root mass between the NF18424 mutant with five leaflets, NF18424 mutant with four leaflets per leaf (one leaflet removed), NF18424 mutant with three leaflets per leaf (two leaflets removed), the NF18424 segregating WT and the R108 WT, all inoculated with *Rhizophagus irregularis* at one time point (5 weeks post planting). Error bars indicate standard error, n = 18.

CHAPTER FOUR

Discussion & Conclusion

4.1 NAC-TF’s involvement in arbuscular mycorrhizal symbiosis

The putative NAC-TF gene *Medtr7g100990* belongs to a large family of plant transcription factors primarily involved in regulating the secretion of defence hormones. We conducted two symbiosis assays to determine if the NAC-TF protein is involved in regulating mycorrhizal symbiosis by assessing the colonization of the model legume *Medicago truncatula* inoculated with *Rhizophagus irregularis*. The *Medtr7g100990* mutant line displayed a significant decrease in mean root length colonization in one (**Figure 3.2.2**) of the two NF18398 symbiosis assays (**Figure 3.3.2-3.3.3**), at 6 wpp.

In addition, we conducted one root phenotyping assay where we measured various morphological features of the NAC-TF *Medicago truncatula* mutants to determine if they display a quantifiable phenotype. Our measurements did not detect any statistically significant difference between the length of longest root, total root length, the number of root tips, fresh root mass, fresh shoot mass, total fresh mass, total dry mass, dry shoot mass and dry root mass of the NF18398 mutant compared to the controls (**Figure 3.3.1-3.3.9**).

Although there was increased expression of the NAC-TF gene *Medtr7g100990* during AM fungal symbiosis, our data does not indicate that this gene plays a clear role in regulating the plant-fungal symbiosis. While we are confident that the allele in NF18398 is a true mutant (as the *Tnt1* insertion is located within a coding region), possible reasons for these inconsistencies between experiments and our inability to observe a phenotype include natural variability (Section 4.3.1), and fully/partially redundant involvement (Section 4.3.2).

Despite a significant decrease in mean root length colonization at 6 wpp in the first NF18398 assay, this trend was not reproduced in the second assay and further research is required before we can reach a definitive conclusion regarding the involvement of

Medtr7g100990 in AM symbiosis. One next step in the study of the NAC-TF mutant involves conducting a third symbiosis assay to further assess the reproducibility of the observed trend. Until then, we cannot conclude whether the gene in question plays a mechanistic role in regulating AM fungal symbiosis prior to and/or during root infection.

4.2 *PALM1*'s involvement in arbuscular mycorrhizal symbiosis

The second gene under study, *PALM1*, has been reported to play a role in the regulation of the trifoliate leaf structure of *M. truncatula* (Chen et al., 2010). We conducted three symbiosis assays and two leaf excision symbiosis assays to investigate whether PALM1 plays a role in the regulation of interactions between the plant host and the fungal symbiont. The *Medtr5g014400* Tnt1 mutant displayed a significant increase in mean root length colonization in all five symbiosis assays (**Figure 3.2.4-3.2.8**). Specifically, the *PALM1* mutant demonstrated a significant increase in mean root colonization at 4 wpp in the first assay (**Figure 3.2.4**), 4 and 5 wpp in the second assay (**Figure 3.2.5**), as well as 2.5 and 4 wpp in the third assay (**Figure 3.2.6**). The data from the first leaf excision assay indicated a significant increase in mean root length colonization for the five-leaflet and four-leaflet mutants at 2, 5, and 6 wpp (**Figure 3.2.7**). The second assay indicated a significant increase in mean root length colonization for the five-leaflet and four-leaflet mutants at 5 and 6 wpp (**Figure 3.2.8**).

Additionally, we took multiple morphological measurements throughout the second leaf-excision assay, including an estimation of total leaf surface area at three timepoints, total fresh mass, fresh shoot mass, fresh root mass, and dry shoot mass at one timepoint (**Figure 3.4.1-3.4.5**). We observed a significant decrease in leaf surface area of the three-leaflet mutant when compared to the controls at 2, 5 and 6 wpp. We did not detect any statistical differences between the mutants and the controls for any of the excised plant's additional measurements.

We also conducted one root phenotyping assay where we measured morphological features of *PALM1 Medicago truncatula* mutants to identify any measurable phenotypes. Our data indicates significantly increased dry root mass (**Figure 3.3.16**) and significantly decreased dry shoot mass (**Figure 3.3.17**). We did not detect a statistically significant difference between the length of longest root, total root length, number of root tips, fresh root mass, fresh shoot mass, total fresh mass, and total dry mass, of the NF18424 mutant compared to the controls (**Figure 3.3.10-3.3.18**).

Our data supports our hypothesis that PALM1 plays a role in regulating AM fungal symbiosis prior to and/or during root infection, resulting in the observed difference in mean root length colonization. This data raises the question of the mechanism by which PALM1 modulates root colonization. One hypothesis is that *PALM1* indirectly affects root colonization by regulating leaf development, whereby the abnormal five-lobed leaf structure in the *PALM1* mutant enhances photosynthetic capacity by increasing total leaf surface area, allowing the plant to allocate more resources to the AM fungus. An alternative hypothesis is that *PALM1* has an undefined role in regulating root development, thereby indirectly suppressing symbioses, where the increased root mass of the mutant increases the opportunity to engage in symbioses.

Based on this study's results, further research into the role of *PALM1* and AM symbiosis is warranted. Future investigation not within the scope of this thesis includes quantifying expression levels of the *PALM1* gene at different time points. By using reference genes as endogenous controls, the relative expression of a target gene by qPCR can be calculated.

An additional experiment planned for the near future includes cloning the promoter region Using Gateway™ cloning technology to investigate *PALM1* promoter activity. When the *Escherichia coli* beta-glucuronidase (GUS) reporter gene is expressed, promoter activity may be observed (Jefferson et al., 1987), and the spatial and temporal expression patterns of the *PALM1* gene may be studied by performing transient *Agrobacterium rhizogenes*-mediated root transformations in *M. truncatula*.

A final experiment includes overexpressing *PALM1* in roots. If a *PALM1* mutant has increased colonization, we might expect that over-expression of this gene in roots will decrease colonization. As we would only genetically transform the roots (and not shoots) to over-express *PALM1*, this may also allow us to separate the role of PALM1 in leaf development versus a role that is root specific.

4.3 General discussion

In this study, we assessed two candidate host genes for potential involvement in regulating arbuscular mycorrhizal symbiosis. In this way, we have contributed towards advancing knowledge of an important and key symbiotic partnership, as determining the possible roles of these genes in plant-fungal symbiosis may have important implications to our global ecosystem. Specifically, we have investigated the potential involvement of two *M. truncatula* genes in AM symbiosis: a gene encoding a putative NAC-TF, and the *PALM1* gene. The results of these symbiosis assays revealed the *PALM1* gene to have a clear role in regulating AM fungal colonization, requiring additional research to further explore the gene's function, whereas the NAC-TF mutant lines displayed an inconsistent phenotype.

4.3.1 Variability

We observed some variability within biological replicates in the symbiosis and root phenotyping experiments, which was depicted by standard error bars. Tremendous care was taken to ensure that every biological replicate was given the exact same treatment conditions, and replicates were always randomly placed in the growth chamber. Slight variances in the availability of light due to the positioning of each replicate and spatial non-uniformity in the growth chamber, and variations in the plants' nutritional status might all be sources of variation (Ji & Bever, 2016). Moreover, while great care was taken to ensure the genotype of all plants in our assays, we cannot exclude the possibility of any cross-contamination of genotypes given the high number of plants assayed. For NF18398, a transgenic line without an observable phenotype, we genotyped 50% of plants assayed (corresponding to 108 plants in total), however it was deemed impractical to genotype all plants within these experiments.

4.3.2 Potential for gene redundancy

The genes we examined could be wholly or partly functionally redundant. There are various instances of genes that are partly redundant in AM symbiosis yet are still involved (An et al., 2019; Maillet et al., 2011). For example, the LysM receptor-like kinase encoded by the MtNFP gene is upstream of the common SYM pathway and contributes to the host's perception of fungal lipochitooligosaccharides (Maillet et al., 2011), although, the MtNFP mutant's symbiotic phenotype is comparable to wild-type controls (Armor et al., 2003). Moreover, mutant knockouts of this gene did not result in a statistically significant difference in colonization or arbuscule abundance of *M. truncatula* inoculated with *R. irregularis* at 5 wpp (An et al., 2019).

According to An et al. (2019), a gene knockout might not be enough to demonstrate a statistically significant phenotype of decreased colonization. A double mutant deletion of two genes that are redundant, or of genes that encode proteins that act upstream or downstream of one another (such as PHANTASTICA (*PHAN*) and ARGONAUTE7 (*AGO7*) pathways discussed in section 1.6.2), might provide valuable information in addition to an over-expression experiment.

4.3.3 Implications of this study

The results of this research may have significant ramifications for comprehending the interactions between the two partners in this crucial relationship for the environment. For example, *PALM1* mutants and arbuscular mycorrhizal fungi could be used in tandem to modulate the rate of fungal colonization in agriculture, which would potentially allow for decreased use of chemical fertilizers. Future research (discussed in section 4.2) that will be conducted by the MacLean laboratory may help to further elaborate the relationship between PALM1 and AM symbiosis, aiding to inform modern farming techniques.

4.3.4 Conclusions

Evidence suggests that the earliest land plants were able to colonize land due to the long-standing mutually beneficial interaction between plants and AM fungus (Rich et al., 2021). The nutrients that AM fungi provide to plants contribute greatly to enhancing worldwide plant nutrition, making AM symbiosis a crucial element that support global plant health and agriculture (Zhang et al., 2016; Koide & Elliott, 1989). Notwithstanding the importance of this mutualism, many of the genes that contribute to the plant-fungal mutualism are still poorly characterized. To further enhance our understanding of the arbuscular mycorrhizal fungal-plant symbiosis, two *Medicago truncatula* genes that we hypothesized to be involved in this mutualism were screened by measuring mean root length colonization by the model AM fungal species *Rhizophagus irregularis*. One gene, a putative NAC-TF, yielded inconclusive results, where future repetition of the symbiosis assays conducted within this research is required. Data obtained for the second gene, *PALM1*, supports a role of the encoded regulator in controlling AM symbioses, and additional research ongoing in the MacLean lab will further determine its role in the symbiosis.

Works Cited

Alonso, Stepanova, A. N., Leisse, T. J., Kim, C. J., Chen, H., Shinn, P., Stevenson, D. K., Zimmerman, J., Barajas, P., Cheuk, R., Gadrinab, C., Heller, C., Jeske, A., Koesema, E., Meyers, C. C., Parker, H., Prednis, L., Ansari, Y., Choy, N., … Ecker, J. R. (2003). Genome-Wide Insertional Mutagenesis of Arabidopsis thaliana. *Science (American Association for the Advancement of Science)*, **301**(5633), 653–657.

An, Zeng, T., Ji, C., Graaf, de, Zheng, Z., Xiao, T. T., Deng, X., Xiao, S., Bisseling, T., Limpens, E., & Pan, Z. (2019). A Medicago truncatula SWEET transporter implicated in arbuscule maintenance during arbuscular mycorrhizal symbiosis. *The New Phytologist*, **224**(1), 396–408.

Bago, Zipfel, W., Williams, R. M., Jeongwon Jun, Arreola, R., Lammers, P. J., Pfeffer F, P. E., & Shachar-Hill, Y. (2002). Translocation and Utilization of Fungal Storage Lipid in the Arbuscular Mycorrhizal Symbiosis. *Plant Physiology (Bethesda)*, **128**(1), 108–124.

Basu, Rabara, R. C., & Negi, S. (2018). AMF: The future prospect for sustainable agriculture. *Physiological and Molecular Plant Pathology*, **102**, 36–45.

Bagyaraj, Sharma, M., & Maiti, D. (2015). Phosphorus nutrition of crops through arbuscular mycorrhizal fungi. *Current Sci.*, **108**(7), 1288-1293.

Barker, Bianchi, S., Blondon, F., Dattee, Y., Duc, G., Essad, S., Flament, P., Gallusci, P., Genier, G., & Guy, P. (1990). Medicago truncatula, a model plant for studying the molecular genetics of the Rhizobium-legume symbiosis. *Plant Molecular Biology Reporter*, **8**(1), 40–49.

Begum, N., Qin, C., Ahanger, M. A., Raza, S., Khan, M. I., Ashraf, M., Ahmed, N., & Zhang, L. (2019). Role of Arbuscular Mycorrhizal Fungi in Plant Growth Regulation: Implications in Abiotic Stress Tolerance. *Frontiers in Plant Science*, **10**, 1068–1068.

Beman, Arrigo, K. R., & Matson, P. A. (2005). Agricultural runoff fuels large phytoplankton blooms in vulnerable areas of the ocean. *Nature*, **434**(7030), 211–214.

Benedito, Torres-Jerez, I., Murray, J. D., Andriankaja, A., Allen, S., Kakar, K., Wandrey, M., Verdier, J., Zuber, H., Ott, T., Moreau, S., Niebel, A., Frickey, T., Weiller, G., He, J., Dai, X., Zhao, P. X., Tang, Y., & Udvardi, M. K. (2008). A gene expression atlas of the model legume Medicago truncatula. *The Plant Journal : for Cell and Molecular Biology*, **55**(3), 504–513.

Berruti, Lumini, E., Balestrini, R., & Bianciotto, V. (2015). Arbuscular Mycorrhizal Fungi as Natural Biofertilizers: Let's Benefit from Past Successes. *Frontiers in Microbiology*, **6**, 1559–1559.

Bhargava, Carmona, F. F., Bhargava, M., & Srivastava, S. (2012). Approaches for enhanced phytoextraction of heavy metals. *Journal of Environmental Management*, **105**, 103–120.

Bonfante, & Venice, F. (2020). Mucoromycota: going to the roots of plant-interacting fungi. *Fungal Biology Reviews,* **34**(2), 100–113.

Ite, Borde, M. Y., & Dudhane, M. P. (2009). Role of Bioinoculant (AM Fungi) Increasing in Growth, Flavor Content and Yield in Allium sativum L. under Field Condition. *Notulae Botanicae Horti Agrobotanici Cluj-Napoca*, **37**(2), 124–124.

Bravo, A., York, T., Pumplin, N., Mueller, L. A., & Harrison, M. J. (2016). Genes conserved for arbuscular mycorrhizal symbiosis identified through phylogenomics. *Nature plants*, **2**, 15208.

Breuillin-Sessoms, Floss, D. S., Gomez, S. K., Pumplin, N., Ding, Y., Levesque-Tremblay, V., Noar, R. D., Daniels, D. A., Bravo, A., Eaglesham, J. B., Benedito, V. A., Udvardi, M. K., & Harrison, M. J. (2015). Suppression of Arbuscule Degeneration in Medicago truncatula phosphate transporter4 Mutants Is Dependent on the Ammonium Transporter 2 Family Protein AMT2;3. *The Plant Cell*, **27**(4), 1352–1366.

Brundrett. (1996). Working with mycorrhizas in forestry and agriculture. Australian Centre for International Agricultural Research.

Carpio, Lucila Amaya, Fred T. Davies, & Michael A Arnold. (2003). Effect of Commercial Arbuscular Mycorrhizal Fungi on Growth, Survivability, and Subsequent Landscape Performance of Selected Container Grown Nursery Crops. *Journal of Environmental Horticulture*, **21**(4): 190–195.

Chabi Sika, K., Kefela, T., & Adoukonou-Sagbadja, H. (2015). A simple and efficient genomic DNA extraction protocol for large scale genetic analyses of plant biological systems. *Plant Gene* **1**: 43–45.

Chen, Mathieu, S., Hoffrichter, A., Sedzielewska-Toro, K., Peart, M., Pelin, A., Ndikumana, S., Ropars, J., Dreissig, S., Fuchs, J., Brachmann, A., & Corradi, N. (2018). Single nucleus sequencing reveals evidence of inter-nucleus recombination in arbuscular mycorrhizal fungi. *eLife*, **7**.

Chen, Morin, E., Beaudet, D., Noel, J., Yildirir, G., Ndikumana, S., Charron, P., St-Onge, C., Giorgi, J., Krüger, M., Marton, T., Ropars, J., Grigoriev, I. V., Hainaut, M., Henrissat, B., Roux, C., Martin, F., & Corradi, N. (2018). High intraspecific genome diversity in the model arbuscular mycorrhizal symbiont Rhizophagus irregularis. *The New Phytologist*, **220**(4), 1161–1171.

Chen, Yu, J., Ge, L., Wang, H., Berbel, A., Liu, Y., Chen, Y., Li, G., Tadege, M., Wen, J., Cosson, V., Mysore, K. S., Ratet, P., Madueño, F., Bai, G., & Chen, R. (2010). Control of dissected leaf morphology by a Cys(2)His(2) zinc finger transcription factor in the model legume Medicago truncatula. *Proceedings of the National Academy of Sciences - PNAS*, **107**(23), 10754–10759.

Cheng, X., Wen, J., Tadege, M., Ratet, P., & Mysore, K.S. (2011). Reverse Genetics in Medicago truncatula Using Tnt1 Insertion Mutants. *Methods in molecular biology*, **678,** 179–190.

Choi, Summers, W., & Paszkowski, U. (2018). Mechanisms Underlying Establishment of Arbuscular Mycorrhizal Symbioses. *Annual Review of Phytopathology*, **56**(1), 135–160.

Christie, Li, X., & Chen, B. (2004). Arbuscular mycorrhiza can depress translocation of zinc to shoots of host plants in soils moderately polluted with zinc. *Plant and Soil*, **261**(1/2), 209–217.

Codd, Lindsay, J., Young, F. M., Morrison, L. F., & Metcalf, J. S. (n.d.). Harmful Cyanobacteria: From mass mortalities to management measures. In *Harmful Cyanobacteria* (pp. 1–23). Springer Netherlands.

Conley, Paerl, H. W., Howarth, R. W., Boesch, D. F., Seitzinger, S. P., Havens, K. E., Lancelot, C., & Likens, G. E. (2009). Controlling Eutrophication: Nitrogen and Phosphorus. *Science (American Association for the Advancement of Science)*, **323**(5917), 1014–1015.

Cook D.R. (1999) Medicago truncatula – a model in the making! *Curr. Opin. Plant Biol*., **2**, 301–304.

Cosme, Fernández, I., Van der Heijden, M. G. ., & Pieterse, C. M. . (2018). Non-Mycorrhizal Plants: The Exceptions that Prove the Rule. *Trends in Plant Science*, **23**(7), 577–587.

Cozzolino, Di Meo, V., & Piccolo, A. (2013). Impact of arbuscular mycorrhizal fungi applications on maize production and soil phosphorus availability. *Journal of Geochemical Exploration*, **129**, 40–44.

Douds, & Schenck, N. C. (1990). Cryopreservation of Spores of Vesicular-Arbuscular Mycorrhizal Fungi. *The New Phytologist*, **115**(4), 667–674.

Ernst, Nina Olsen, A., Skriver, K., Larsen, S., & Lo Leggio, L. (2004). Structure of the conserved domain of ANAC, a member of the NAC family of transcription factors. *EMBO Reports*, **5**(3), 297–303.

Ezawa, T., & Saito, K. (2018). How do arbuscular mycorrhizal fungi handle phosphate? New insight into fine-tuning of phosphate metabolism. *New Phytologist*, **220**(4), 1116–1121.

Faye, Dalpé, Y., Ndung'u-Magiroi, K., Jefwa, J., Ndoye, I., Diouf, M., & Lesueur, D. (2013). Evaluation of commercial arbuscular mycorrhizal inoculants. *Canadian Journal of Plant Science*, **93**(6), 1201–1208.

Feng, Sun, J., Radhakrishnan, G. V., Lee, T., Bozsóki, Z., Fort, S., Gavrin, A., Gysel, K., Thygesen, M. B., Andersen, K. R., Radutoiu, S., Stougaard, J., & Oldroyd, G. E. D. (2019). A combination of chitooligosaccharide and lipochitooligosaccharide recognition promotes arbuscular mycorrhizal associations in Medicago truncatula. *Nature Communications*, **10**(1), 5047–12.

Fried, S., Mackie, B., & Nothwehr, E. (2012). Nitrate and phosphate levels positively affect the growth of algae species found in Perry Pond. Tillers, **4**, 21-24. Retrieved from https://ojs.grinnell.edu/index.php/tillers/article/view/33

García-Garrido, & Ocampo, J. A. (2002). Regulation of the plant defence response in arbuscular mycorrhizal symbiosis. *Journal of Experimental Botany*, **53**(373), 1377–1386.

Ge, Peng, J., Berbel, A., Madueno, F., & Chen, R. (2014). Regulation of Compound Leaf Development by PHANTASTICA in Medicago truncatula. *Plant Physiology (Bethesda)*, **164**(1), 216–228.

Ge, Chen, J., & Chen, R. (2010). Palmate-like pentafoliata1 encodes a novel Cys(2)His(2) zinc finger transcription factor essential for compound leaf morphogenesis in Medicago truncatula. *Plant Signaling & Behavior*, **5**(9), 1134–1137.

Genre, & Bonfante, P. (2005). Building a mycorrhizal cell: How to reach compatibility between plants and arbuscular mycorrhizal fungi. *Journal of Plant Interactions*, **1**(1), 3–13.

Genre, Chabaud, M., Balzergue, C., Puech-Pagès, V., Novero, M., Rey, T., Fournier, J., Rochange, S., Bécard, G., Bonfante, P., & Barker, D. G. (2013). Short-chain chitin oligomers from arbuscular mycorrhizal fungi trigger nuclear Ca2+ spiking in Medicago truncatula roots and their production is enhanced by strigolactone. *The New Phytologist*, **198**(1), 179–189.

Gianinazzi-Pearson. (1996). Plant cell responses to arbuscular mycorrhizal fungi: getting to the roots of the symbiosis. *The Plant Cell*, **8**(10), 1871–1883.

Giovannetti, & Mosse, B. (1980). An Evaluation of Techniques for Measuring Vesicular Arbuscular Mycorrhizal Infection in Roots. *The New Phytologist*, ***84***(3), 489–500.

Grman. (2012). Plant species differ in their ability to reduce allocation to non-beneficial arbuscular mycorrhizal fungi. *Ecology (Durham),* **93**(4), 711–718.

Gruber, V., Blanchet, S., Diet, A., Zahaf, O., Boualem, A., Kakar, K., Alunni, B., Udvardi, M., Frugier, F. and Crespi, M. (2009) Identification of transcription factors involved in root apex responses to salt stress in Medicago truncatula. *Mol. Genet. Genomics*, **281**, 55–66.

Gutjahr, & Parniske, M. (2017). Cell Biology: Control of Partner Lifetime in a Plant–Fungus Relationship. *Current Biology*, **27**(11), R420–R423.

Harrier, & Millam, S. (2001). Biolistic transformation of arbuscular Mycorrhizal fungi : Progress and perspectives. *Molecular Biotechnology*, 18(1), 25–33.

Harrier. (2000). Arbuscular Mycorrhizal (AM) Symbiosis: A Review of Signalling and Molecular Aspects of Root Colonisation. *Botanical Journal of Scotland*, **52**(2), 159–169.

He, Benedito, V. A., Wang, M., Murray, J. D., Zhao, P. X., Tang, Y., & Udvardi, M. K. (2009). The Medicago truncatula gene expression atlas web server. *BMC Bioinformatics*, **10**(1), 441–441.

He, L., Liu, Y., He, H., Liu, Y., Qi, J., Zhang, X., Li, Y., Mao, Y., Zhou, S., Zheng, X., Bai, Q., Zhao, B., Wang, D., Wen, J., Mysore, K. S., Tadege, M., Xia, Y., & Chen, J. (2020). A molecular framework underlying the compound leaf pattern of Medicago truncatula. *Nature plants*, **6**(5), 511–521.

Heinemeyer, A., & Fitter, A.H. (2004). Impact of temperature on the arbuscular mycorrhizal (AM) symbiosis: growth responses of the host plant and its AM fungal partner. *Journal of Experimental Botany*, **55**(396): 525-534.

Hoagland, D., & Arnon, D. (1950). The water-culture method for growing plants without soil: Internet Archive. Berkeley: College of Agriculture, University of California.

Hussey, Saïdi, M. N., Hefer, C. A., Myburg, A. A., & Grima-Pettenati, J. (2015). Structural, evolutionary and functional analysis of the NAC domain protein family in Eucalyptus. *The New Phytologist*, **206**(4), 1337–1350.

Javot, H., Pumplin, N., & Harrison, M. J. (2007). Phosphate in the arbuscular mycorrhizal symbiosis: Transport properties and regulatory roles. *Plant, Cell and Environment*, **30**(3).

Jefferson, Kavanagh, T.A., & Bevan M.W. (1987). GUS fusions: B-glucuronidase as a sensitive and versatile gene fusion marker in higher plants. *The EMBO Journal*, **6**, 3901-3907.

Ji, & Bever, J. D. (2016). Plant preferential allocation and fungal reward decline with soil phosphorus: Implications for mycorrhizal mutualism. *Ecosphere (Washington, D.C)*, **7**(5).

Jiang, Wang, W., Xie, Q., Liu, N., Liu, L., Wang, D., Zhang, X., Yang, C., Chen, X., Tang, D., & Wang, E. (2017). Plants transfer lipids to sustain colonization by mutualistic mycorrhizal and parasitic fungi. *Science (American Association for the Advancement of Science),* **356**(6343), 1172–1175.

Joner, Briones, R., & Leyval, C. (2000). Metal-binding capacity of arbuscular mycorrhizal mycelium. Plant and Soil, 226(2), 227–234.Kapulnik, Volpin, H., Itzhaki, H., Ganon, D., Galili, S., David, R., Shaul, O., Elad, Y., Chet, I., & Okon, Y. (1996). Suppression of Defence Responses in Mycorrhizal Alfalfa and Tobacco Roots. *New Phytologist*, **133**(1), 59–64.

Kiers, Duhamel, M., Beesetty, Y., Mensah, J. A., Franken, O., Verbruggen, E., Fellbaum, C. R., Kowalchuk, G. A., Hart, M. M., Bago, A., Palmer, T. M., West, S. A., Vandenkoornhuyse, P., Jansa, J., & Bücking, H. (2011). Reciprocal Rewards Stabilize Cooperation in the Mycorrhizal Symbiosis. *Science (American Association for the Advancement of Science),* **333**(6044), 880–882.

Kistner, & Parniske, M. (2002). Evolution of signal transduction in intracellular symbiosis. *Trends in Plant Science*, **7**(11), 511–518.

Kloppholz, Kuhn, H., & Requena, N. (2011). A Secreted Fungal Effector of Glomus intraradices Promotes Symbiotic Biotrophy. *Current Biology*, **21**(14), 1204–1209.

Koide, & Elliot, G. (1989). Cost, Benefit and Efficiency of the Vesicular-Arbuscular Mycorrhizal Symbiosis. *Functional Ecology*, **3**(2), 252–255.

Kokkoris, Li, Y., Hamel, C., Hanson, K., & Hart, M. (2019). Site specificity in establishment of a commercial arbuscular mycorrhizal fungal inoculant. *The Science of the Total Environment*, **660**, 1135–1143.

Krajinski, Courty, P.-E., Sieh, D., Franken, P., Zhang, H., Bucher, M., Gerlach, N., Kryvoruchko, I., Zoeller, D., Udvardi, M., & Hause, B. (2014). The H+-ATPase HA1 of Medicago truncatula Is Essential for Phosphate Transport and Plant Growth during Arbuscular Mycorrhizal Symbiosis. *The Plant Cell*, **26**(4), 1808–1817.

Lanfranco, Bonfante, P., & Genre, A. (2016). The Mutualistic Interaction between Plants and Arbuscular Mycorrhizal Fungi. *Microbiology Spectrum*, **4**(6).

Le, D.T., Nishiyama, R., Watanabe, Y., Mochida, K., Yamaguchi-Shinozaki, K., Shinozaki, K., et al. (2011). Genome-wide survey and expression analysis of the plant-specific

NAC transcription factor family in soybean during development and dehydration stress. DNA Res. **18**, 263–276.

Leigh, J., Hodge, A., & Fitter, A. H. (2009). Arbuscular mycorrhizal fungi can transfer substantial amounts of nitrogen to their host plant from organic material. New Phytol. **181**, 199–207.

Leghari, S.J., Wahocho, N.A., Laghari, G.M., & (2016). Role of Nitrogen for Plant Growth and Development: A review. Advances in Environmental Biology. 10. 209-218.

Li, B., Boiarkina, I., Young, B., Yu, W., & Singhal, N. (2017). Prediction of Future Phosphate Rock: A Demand Based Model. *Journal of Environmental Informatics*, **31**(1), 41-53.

Ling, L., Song, L., Wang, Y., & Guo, C. (2017). Genome-wide analysis and expression patterns of the NAC transcription factor family in Medicago truncatula. *Physiology and molecular biology of plants: an international journal of functional plant biology*, **23**(2), 343–356.

López-Ráez, Pozo, M. J., & García-Garrido, J. M. (2011). Strigolactones: a cry for help in the rhizosphere. *Botany*, **89**(8), 513–522.

MacLean, Bravo, A., & Harrison, M. J. (2017). Plant Signaling and Metabolic Pathways Enabling Arbuscular Mycorrhizal Symbiosis. *The Plant Cell*, **29**(10), 2319–2335.

Maillet, Poinsot, V., Andres Martinez, E., Driguez, H., Becard, G., Denaire, J., Andre, O., Puech-Pages, V., Haouy, A., Gueunier, M., Cromier, L., Giraudet, D., Formey, D., & Niebel, A. (2011). Fungal lipochitooligosaccharide symbiotic signals in arbuscular mycorrhiza. *Nature (London), 469*(7328), 58–63.

Mao, Zhang, H., Qian, X., Li, A., Zhao, G., & Jing, R. (2012). TaNAC2, a NAC-type wheat transcription factor conferring enhanced multiple abiotic stress tolerances in Arabidopsis. *Journal of Experimental Botany*, **63**(8), 2933–2946.

Menge. (1983). Utilization of vesicular-arbuscular mycorrhizal fungi in agriculture. *Canadian Journal of Botany*, **61**(3), 1015–1024.

Miyata, Kozaki, T., Kouzai, Y., Ozawa, K., Ishii, K., Asamizu, E., Okabe, Y., Umehara, Y., Miyamoto, A., Kobae, Y., Akiyama, K., Kaku, H., Nishizawa, Y., Shibuya, N., & Nakagawa, T. (2014). The bifunctional plant receptor, OsCERK1, regulates both chitin-triggered immunity and arbuscular mycorrhizal symbiosis in rice. *Plant and Cell Physiology*, **55**(11), 1864–1872.

Montero, H., Choi, J., & Paszkowski, U. (2019). Arbuscular mycorrhizal phenotyping: the dos and don’ts. *New Phytology* **221**(3): 1182–1186.

Neset, & Cordell, D. (2012). Global phosphorus scarcity: identifying synergies for a sustainable future. *Journal of the Science of Food and Agriculture*, **92**(1), 2–6.

Oldroyd, & Downie, J. A. (2006). Nuclear calcium changes at the core of symbiosis signalling. *Current Opinion in Plant Biology*, **9**(4), 351–357.

Parniske. (2008). Arbuscular mycorrhiza: the mother of plant root endosymbioses. Nature Reviews. *Microbiology*, **6**(10), 763–775.

Paszkowski. (2006). A Journey through Signaling in Arbuscular Mycorrhizal Symbioses 2006. *The New Phytologist*, **172**(1), 35–46.

Pinheiro, Marques, C. S., Costa, M. D. B. ., Reis, P. A. ., Alves, M. S., Carvalho, C. M., Fietto, L. G., & Fontes, E. P. (2009). Complete inventory of soybean NAC transcription factors: Sequence conservation and expression analysis uncover their distinct roles in stress response. *Gene*, **444**(1), 10–23.

Pirozynski, & Malloch, D. . (1975). The origin of land plants: A matter of mycotrophism. *BioSystems*, **6**(3), 153–164.

Roy-bolduc, Alice, & Hijri, Mohamed. (2011). The Use of Mycorrhizae to Enhance Phosphorus Uptake : A Way Out The Phosphorus Crisis. *Journal of Biofertilizers & Biopesticides*, **2**(1): 1–5.

Parniske, M. (2008). Arbuscular mycorrhiza: The mother of plant root endosymbioses. *Nature Reviews Microbiology*, **6**(10), 763–775.

Peng, Berbel, A., Madueño, F., & Chen, R. (2017). AUXIN RESPONSE FACTOR3 regulates compound leaf patterning by directly repressing PALMATE-LIKE PENTAFOLIATA1 expression in medicago truncatula. *Frontiers in Plant Science*, **8**, 1630–1630.

Pumplin, N., & Harrison, M. J. (2009). Live-cell imaging reveals periarbuscular membrane domains and organelle location in Medicago truncatula roots during arbuscular mycorrhizal symbiosis. *Plant Physiology*, **151**, 809–819.

Puranik, Sahu, P. P., Srivastava, P. S., & Prasad, M. (2012). NAC proteins: regulation and role in stress tolerance. *Trends in Plant Science*, **17**(6), 369–381.

Redecker, Kodner, R., & Graham, L. E. (2000). Glomalean Fungi from the Ordovician. *Science (American Association for the Advancement of Science)*, **289**(5486), 1920–1921.

Remy, Taylor, T. N., Hass, H., & Kerp, H. (1994). Four Hundred-Million-Year-Old Vesicular Arbuscular Mycorrhizae. *Proceedings of the National Academy of Sciences - PNAS*, **91**(25), 11841–11843.

Rich, Vigneron, N., Libourel, C., Keller, J., Xue, L., Hajheidari, M., Radhakrishnan, G. V., Le Ru, A., Diop, S. I., Potente, G., Conti, E., Duijsings, D., Batut, A., Le Faouder, P., Kodama, K., Kyozuka, J., Sallet, E., Bécard, G., Rodriguez-Franco, M., … Delaux, P.-M. (2021). Lipid exchanges drove the evolution of mutualism during plant terrestrialization. *Science (American Association for the Advancement of Science)*, **372**(6544), 864–868.

Rosikiewicz, Bonvin, J., & Sanders, I. R. (2017). Cost-efficient production of in vitro Rhizophagus irregularis. *Mycorrhiza*, **27**(5), 477–486.

Roth, & Paszkowski, U. (2017). Plant carbon nourishment of arbuscular mycorrhizal fungi. *Current Opinion in Plant Biology*, **39**, 50–56.

Sanders. (2003). Preference, specificity and cheating in the arbuscular mycorrhizal symbiosis. *Trends in Plant Science*, **8**(4), 143–145.

Sato, T., Hachiya, S., Inamura, N., Ezawa, T., Cheng, W., & Tawaraya, K. (2019). Secretion of acid phosphatase from extraradical hyphae of the arbuscular mycorrhizal fungus Rhizophagus clarus is regulated in response to phosphate availability. *Mycorrhiza*, **29**, 599–605.

Schüßler A, 2017. AMF species list 190530. Retrieved from: http://www.amfphylogeny.com/amphylo_species.html?fbclid=IwAR034_N9D_9u6y0HHov3VoZi5bC5RhSVDl6_e_l6eLbP_J6CZnsZLckxi2k

Seddas, P. M., Arias, C. M., Arnould, C., van Tuinen, D., Godfroy, O., Benhassou, H. A., Gouzy, J., Morandi, D., Dessaint, F., & Gianinazzi-Pearson, V. (2009). Symbiosis-related plant genes modulate molecular responses in an arbuscular mycorrhizal fungus during early root interactions. *Molecular plant-microbe interactions: MPMI*, **22**(3), 341–351.

Siciliano, Genre, A., Balestrini, R., deWit, P. J. G. M., & Bonfante, P. (2007). Pre-Penetration Apparatus Formation During AM Infection is Associated with a Specific Transcriptome Response in Epidermal Cells. *Plant Signaling & Behavior*, **2**(6), 533–535.

Sun, Chen, W., Ivanov, S., MacLean, A. M., Wight, H., Ramaraj, T., Mudge, J., Harrison, M. J., & Fei, Z. (2019). Genome and evolution of the arbuscular mycorrhizal fungus Diversispora epigaea (formerly Glomus versiforme) and its bacterial endosymbionts. *The New Phytologist*, **221**(3), 1556–1573.

Tadege, M., Wen, J., He, J., Tu, H., Kwak, Y., Eschstruth, A., Cayrel, A., Endre, G., Zhao, P. X., Chabaud, M., Ratet, P., & Mysore, K. S. (2008). Large-scale insertional mutagenesis using the Tnt1 retrotransposon in the model legume Medicago truncatula. *The Plant journal: for cell and molecular biology*, **54**(2), 335–347.

ThermoFisher Scientific, 2009. Wheat Germ Agglutinin Conjugates. Molecular Probes, Inc. Retrieved from: https://www.thermofisher.com/document-connect/documentconnect.html?id=man0001784&version=1.0&pdfurl=https%3A%2F%2Fassets.thermofisher.com

Trieu A.T., Burleigh, S.H., Kardailsky, I.V., Maldonado-Mendoza, I.E., Versaw, W.K., Blaylock, L.A., Shin, H., Chiou, T.-J., Katagi, H., Dewbre, G.R., Weigel, D. and Harrison, M.J. (2000) Transformation of Medicago truncatula via infiltration of seedlings or flowering plants with Agrobacterium. *Plant J.*, **22**, 531–542.

Tran, Nakashima, K., Sakuma, Y., Simpson, S., Fujita, Y., Maruyama, K., Fujita, M., Seki, M., Shinozaki, K., & Yamaguchi-Shinozaki, K. (2004). Isolation and Functional Analysis of Arabidopsis Stress-Inducible NAC Transcription Factors That Bind to a Drought-Responsive cis-Element in the early responsive to dehydration stress 1 Promoter. *The Plant Cell*, **16**(9), 2481–2498.

Trapnell, Roberts, A., Goff, L., Pertea, G., Kim, D., Kelley, D. R., Pimentel, H., Salzberg, S. L., Rinn, J. L., & Pachter, L. (2012). Differential gene and transcript expression analysis of RNA-seq experiments with TopHat and Cufflinks. *Nature Protocols*, **7**(3), 562–578.

Uppalapati, Ishiga, Y., Doraiswamy, V., Bedair, M., Mittal, S., Chen, J., Nakashima, J., Tang, Y., Tadege, M., Ratet, P., Chen, R., Schultheiss, H., & Mysore, K. S. (2012). Loss of Abaxial Leaf Epicuticular Wax in Medicago truncatula irg1/palm1 Mutants Results in Reduced Spore Differentiation of Anthracnose and Nonhost Rust Pathogens. *The Plant Cell*, **24**(1), 353–370.

Vance, C. P., Uhde-Stone, C., & Allan, D. L. (2003). Phosphorus acquisition and use: Critical adaptations by plants for securing a nonrenewable resource. *New Phytologist*, **157**(3), 423–447.

Vierheilig, Schweiger, P., & Brundrett, M. (2005). An overview of methods for the detection and observation of arbuscular mycorrhizal fungi in roots. *Physiologia Plantarum*, **125**(4), 393–404.

Walder F, van der Heijden MGA. (2015). Regulation of resource exchange in the arbuscular mycorrhizal symbiosis. *Nature Plants* **1**, 1–7.

Wang, X. X., Hoffland, E., Feng, G., & Kuyper, T. W. (2017). Phosphate uptake from phytate due to hyphae-mediated phytase activity by arbuscular mycorrhizal maize. *Frontiers in Plant Science*, **8**, 1–8.

Whiteside, Werner, G. D. ., Caldas, V. E. ., van't Padje, A., Dupin, S. E., Elbers, B., Bakker, M., Wyatt, G. A. ., Klein, M., Hink, M. A., Postma, M., Vaitla, B., Noë, R., Shimizu, T. S., West, S. A., & Kiers, E. T. (2019). Mycorrhizal Fungi Respond to Resource Inequality by Moving Phosphorus from Rich to Poor Patches across Networks. *Current Biology*, **29**(12), 2043–2050.e8

Yoshii, Shimizu, T., Yamazaki, M., Higashi, T., Miyao, A., Hirochika, H., & Omura, T. (2009). Disruption of a novel gene for a NAC-domain protein in rice confers resistance to Rice dwarf virus. *The Plant Journal: for Cell and Molecular Biology*, **57**(4), 615–625.

Zélicourt, Diet, A., Marion, J., Laffont, C., Ariel, F., Moison, M., Zahaf, O., Crespi, M., Gruber, V., & Frugier, F. (2012). Dual involvement of a Medicago truncatula NAC transcription factor in root abiotic stress response and symbiotic nodule senescence. *The Plant Journal: for Cell and Molecular Biology*, **70**(2), 220–230.

Zhang, Wang, L., Ma, F., Zhang, X., & Fu, D. (2016). Reducing nitrogen runoff from paddy fields with arbuscular mycorrhizal fungi under different fertilizer regimes. *Journal of Environmental Sciences (China)*, **46**(8), 92–100.

Zhang, Y., Song, G., Lal, N. K., Nagalakshmi, U., Li, Y., Zheng, W., … Dinesh-Kumar, S. P. (2019). TurboID-based proximity labeling reveals that UBR7 is a regulator of N NLR immune receptor-mediated immunity. *Nature Communications*, **10**, 1–17.

Zhong, Demura, T., & Ye, Z.-H. (2006). SND1, a NAC Domain Transcription Factor, Is a Key Regulator of Secondary Wall Synthesis in Fibers of Arabidopsis. *The Plant Cell*, **18**(11), 3158–3170.